

NACA TM 1264

TECH LIBRARY KAFD. NM  
0144694

# NATIONAL ADVISORY COMMITTEE FOR AERONAUTICS

TECHNICAL MEMORANDUM 1264

CALCULATION OF THE LATERAL-DYNAMIC  
STABILITY OF AIRCRAFT

By A. Raikh

Translation

"Raschet Bokovoi Dinamicheskoi Ustoichivosti Samolets." Trudy  
Tsentralnogo Aero-Gidrodinamicheskogo Instituta, No. 453, 1939.



Washington  
February 1952

AFMDC  
TECHNICAL LIBRARY  
1952 2611

7917



iZ

## NATIONAL ADVISORY COMMITTEE FOR AERONAUTICS

## TECHNICAL MEMORANDUM 1264

## CALCULATION OF THE LATERAL-DYNAMIC STABILITY OF AIRCRAFT\*

By A. Raikh

The object of this report is to present a method of computing the lateral-dynamic stability of an airplane.

Graphs and formulas are given with the aid of which all the aerodynamic coefficients required for computing the lateral dynamic stability can be determined. A number of numerical examples are given for obtaining the stability derivatives and solving the characteristic-stability equation. Approximate formulas are derived with the aid of which rapid preliminary computations may be made and the stability coefficients corrected for certain modifications of the airplane. A derivation of the lateral-dynamic-stability equations is included.

## INTRODUCTION

In the present stage of development of airplane design, constantly increasing requirements are imposed on the airplane as regards stability and maneuverability. If the area of the vertical tail surface and the transverse dihedral of the wing are unfavorably chosen, the airplane will be subjected to large lateral motions at the least gust of wind and the pilot will be under the constant necessity of applying the controls. Some airplanes because of their flying qualities are generally approved by pilots. Computations show that such airplanes are spirally unstable only at sufficiently large angles of attack but are spirally stable at small angles of attack.

A method of computation of the lateral-dynamic stability is presented herein. The computation is illustrated by examples of the computation of a Northrup 2E airplane, which has received the highest commendation of pilots for its piloting characteristics with regard to stability and maneuverability.

The difficulty of computing the dynamic stability lies in the fact that a large number of aerodynamic coefficients, the so-called

---

\*"Raschet Bokovoi Dinamicheskoi Ustoichivosti Samolets." Trudy Tsentralnogo Aero-Gidrodinamicheskogo Instituta, No. 453, 1939.

2074

rotary derivatives, are required for the computation. These derivatives are not encountered in the usual aerodynamic computation. In order to facilitate the computation, a number of curves are given with the aid of which these magnitudes are rapidly and simply determined. The numerical examples given for computing the coefficients further simplify the problem.

A comparison of the aerodynamic coefficient obtained by computation from graphs and that determined from tests in the wind tunnel is presented herein. In order to check the accuracy of the final data, a comparison is given of the period of oscillation and the time taken for the damping of the lateral motion as obtained from flight tests and by computation, respectively. The comparison shows that the computation gives good results.

Notwithstanding the apparent complexity, the entire computation on the lateral stability from the available aerodynamic coefficients takes no longer than 1.5 to 2 hours. The author expresses his thanks to A. I. Silman, a candidate for a technical degree, for a number of valuable suggestions utilized in this work.

#### SYSTEM OF AXES AND NOTATION

The system of axes is shown in figure 1. The origin of the coordinates is at the center of gravity of the airplane.

The X-axis is in the plane of symmetry of the airplane and directed parallel to the velocity in steady flight. The Y-axis is perpendicular to the plane of symmetry of the airplane and directed to the right of the pilot. The Z-axis is in the plane of symmetry perpendicular to the X-axis and directed downwards.

X, Y, Z	forces along corresponding axes; positive if direction agrees with direction of axes
L, M, N	moments about corresponding axes: moment L is positive if it causes right wing to drop; moment M is positive if it causes tail to drop; moment N is positive if it causes backward motion of right wing
u, v, w	projections of linear velocity on corresponding axes; positive if direction of projections agrees with directions of axes
P, q, r	projections of angular velocities; have same positive directions as moments L, M, N

2074

$\phi, \theta, \psi$	angles made by given direction with X-, Y-, Z-axes respectively; have same positive directions as L, M, N
A, B, C	moments of inertia about X-, Y-, Z-axes
E	the centrifugal moment of inertia [Ed. note, product of inertia with respect to X- and Y-axis]
$\alpha$	angle of attack, degrees
$\alpha_a$	angle of attack computed from line of zero lift, degrees
$\beta$	sideslip angle, $\beta = -\text{arc sin } v/V$ , radians [NACA comment: $\beta$ as used in this report is of opposite sign to $\beta$ as used in American and British reports.]
$\theta$	angle of inclination of flight path to horizontal (positive for lift), degrees
$\psi$	angle of dihedral of wing, angle between plane of chords and plane at right angles to plane of symmetry and passing through chord at tip, degrees
X	angle of sweepback, angle between focal line at 0.25 chord computed from leading edge and plane perpendicular to axis of fuselage, degrees
x	angle between line joining center of gravity of airplane with geometric center of vertical tail surface (with part of fuselage) and line of zero lift, degrees
S	area of wing
$S_{tf}$	area of vertical tail with part of fuselage (fig. 11)
$S_f$	area of lateral projection of fuselage
b	span

$c_0$	chord at root of wing
$c_t$	chord at tip of wing, effective tip chord is determined by prolonging lines of leading and trailing edges
$\lambda = b^2/S$	aspect ratio
$\eta = c_0/c_t$	taper of wing
$l_{nf}$	distance from nose of fuselage to center of gravity of airplane
$l_t$	distance from rudder hinge to center of gravity
$l_f$	length of fuselage
$\rho$	density of the air
$K_{vt}$	coefficient of effectiveness of vertical tail surface
$C_y = \frac{Y}{\frac{\rho V^2}{2} S}$	coefficient of lateral force
$C_l = \frac{L}{\frac{\rho V^2}{2} Sb}$	coefficient of rolling moment
$C_n = \frac{N}{\frac{\rho V^2}{2} Sb}$	coefficient of yawing moment
$C_L = \frac{L}{\frac{\rho V^2}{2} S}$	lift force coefficient
$y_\beta = \frac{\partial C_y}{\partial \beta}$	nondimensional derivative of lateral force with respect to sideslip angle ( $\beta$ in radians)
$l_\beta = \frac{\partial C_l}{\partial \beta}$	nondimensional derivative of rolling moment with respect to sideslip angle

$$n_{\beta} = \frac{\partial C_n}{\partial \beta}$$

nondimensional derivative of yawing moment with respect to sideslip angle

$$l_p = \frac{\partial C_l}{\partial \frac{pb}{2V}}$$

nondimensional derivative of rolling moment with respect to angular velocity of roll

$$n_p = \frac{\partial C_n}{\partial \frac{pb}{2V}}$$

nondimensional derivative of yawing moment with respect to angular velocity of roll

$$l_r = \frac{\partial C_l}{\partial \frac{rb}{2V}}$$

nondimensional derivative of rolling moment with respect to angular velocity of yaw

$$n_r = \frac{\partial C_n}{\partial \frac{rb}{2V}}$$

nondimensional derivative of yawing moment with respect to angular velocity of yaw

$$i_A = \frac{4A}{mb^2}$$

coefficient of moment of inertia about X-axis

$$i_C = \frac{4C}{mb^2}$$

coefficient of moment of inertia about Z-axis

G

weight of airplane

$$m = \frac{G}{g}$$

mass of airplane

$$\mu = \frac{2m}{\rho S b}$$

relative density of airplane

$$\tau = \frac{m}{\rho S V}$$

unit of time

$$\bar{t} = \frac{t}{\tau}$$

nondimensional time

$A_4, A_3, A_2, A_1, A_0$  coefficients of characteristic equation

## 1. EQUATIONS OF LATERAL-DYNAMIC STABILITY OF AIRPLANE

If the rectilinear steady flight of an airplane is considered, the motion of airplane after a certain disturbance is described by a system of six equations with six variables:

$$u, w, q, \text{ and } \beta, p, r$$

If only small deviations of the airplane from steady rectilinear flight are considered, it may be shown (reference 1) that the system of six differential equations breaks up into two independent systems of equations. In the first system of differential equations the following variables enter:

- u projection of linear velocity on X-axis
- w projection of linear velocity on Z-axis
- q projection of angular velocity on Y-axis

In the first system of equations, there enter only variables characterizing the motion of the airplane in the plane of symmetry (that is in the plane XOZ). In the second group of equations there enter the variables:

- $\beta$  angle of sideslip, determined by projection of velocity on Y-axis (sideslip velocity  $v$ )
- p projection of angular velocity on X-axis
- r projection of angular velocity on Z-axis

The variables  $\beta$ ,  $p$ , and  $r$  characterize the lateral motion of the airplane.

By assuming the nondependence of the lateral motion of the airplane on its longitudinal motion, the equations of the lateral dynamic stability can be derived.

For steady rectilinear flight without sideslip

$$\left. \begin{aligned} X = Y = Z = L = M = N = 0 \\ p = q = r = 0 \\ w = v = 0 \\ u = V \end{aligned} \right\} \quad (1)$$

where  $V$  is the velocity of the airplane.

After a certain lateral disturbance, the magnitudes  $p$ ,  $r$ , and  $v$  will vary with time, whereas the magnitudes  $q$ ,  $w$ , and  $u$  may be considered constant.

Because at the initial instant  $p = r = v = 0$ , the disturbances of the magnitudes  $p$ ,  $r$ , and  $v$  are denoted by the same symbols:

$$\Delta p = p$$

$$\Delta r = r$$

$$\Delta v = v$$

Evidently, the lateral motion of the airplane will be characterized by three equations: (a) the equation of the equilibrium of the forces along the Y-axis, (b) the equation of the equilibrium of the moments of the forces about the X-axis, and (c) the equation of the equilibrium of the forces about the Z-axis. By the fundamental equation of mechanics, the product of the mass of the airplane by the projection of the absolute acceleration on the Y-axis is equal to the projection of all external forces acting on the airplane on the Y-axis.

In the general case, the projection of the absolute acceleration of the Y-axis is equal to (reference 2)

$$\frac{dv}{dt} + ru - pv$$

and the equation of equilibrium of the forces along the Y-axis will be of the form

$$m \left( \frac{dv}{dt} + rv \right) = Y \quad (2)$$

For the case under consideration<sup>1</sup>

$$u = V \quad \text{and} \quad w = 0$$

In equation (2),  $Y$  denotes the sum of the projections on the Y-axis of all the external forces acting on the airplane so that

$$Y = Y_a + Y_w \quad (3)$$

where

$Y_a$  projection of aerodynamic force on Y-axis

$Y_w$  projection of weight on Y-axis

In what follows, it is assumed that the aerodynamic force acting on the airplane during a disturbed motion and the small deviations from the condition of steady rectilinear flight depend linearly on the disturbances, and because at the initial instant no lateral force acted on the airplane the aerodynamic force is given by

$$Y_a = \frac{\partial Y}{\partial v} v + \frac{\partial Y}{\partial p} p + \frac{\partial Y}{\partial r} r$$

If the small magnitudes  $\frac{\partial Y}{\partial p} p$  and  $\frac{\partial Y}{\partial r} r$  are neglected, the following equation is obtained:

$$Y_a = \frac{\partial Y}{\partial v} v \quad (4)$$

In symmetrical flight there are no gravitational forces acting on the airplane along the Y-axis. If the airplane rolls, a component appears on the Y-axis. When small oscillations occur, the force acting along the Y-axis for a rolling angle  $\phi$  is equal to (figs. 2 and 3)

$$G \cos \theta \cdot \phi$$

---

<sup>1</sup>In a rigorous derivation, the term  $p w$  drops out as a magnitude of second order of smallness.

2074

where  $\theta$  is the angle of inclination of the flight path. Similarly, for the rotation of the airplane about the Z-axis by an angle  $\psi$  the component along the Y-axis (fig. 4) is

$$G \sin \theta \psi$$

Hence, for small deviations

$$Y_w = G \cos \theta \Phi + G \sin \theta \cdot \psi = G \cos \theta (\Phi + \tan \theta \psi)$$

But

$$G \cos \theta = C_L \frac{\rho V^2}{2} S$$

Therefore,

$$Y_T = C_L \frac{\rho V^2}{2} S (\Phi + \tan \theta \cdot \psi) \quad (5)$$

For small oscillations of the airplane, it may be assumed that

$$v = -V \sin \beta \approx -V\beta$$

When this relation is taken into account and equations (3), (4), and (5) are substituted in equation (2)

$$mV \left( -\frac{d\beta}{dt} + r \right) = \frac{\partial Y}{\partial \beta} \beta + C_L \frac{\rho V^2}{2} S (\Phi + \tan \theta \cdot \psi) \quad (6)$$

The equations of equilibrium of the moments about the X- and Z-axes are of the form (reference 3)

$$\begin{aligned} A \frac{dp}{dt} - E \frac{dr}{dt} &= L \\ C \frac{dr}{dt} - E \frac{dp}{dt} &= N \end{aligned} \quad (7)$$

The moments of the aerodynamic forces  $L$  and  $N$  on the free motion<sup>2</sup> of the airplane after a disturbance will depend on the angular velocities  $p$  and  $r$  and the angle of sideslip  $\beta$ . For the small disturbances  $p$ ,  $r$ , and  $\beta$ , the aerodynamic moments may be represented as follows by a linear dependence on  $p$ ,  $r$ , and  $\beta$ .

---

<sup>2</sup>The free motion of the airplane after a disturbance with locked controls.

$$L = \frac{\partial L}{\partial \beta} \beta + \frac{\partial L}{\partial p} p + \frac{\partial L}{\partial r} r$$

$$N = \frac{\partial N}{\partial \beta} \beta + \frac{\partial N}{\partial p} p + \frac{\partial N}{\partial r} r$$

Equations (7) now become

$$\left. \begin{aligned} A \frac{dp}{dt} - E \frac{dr}{dt} &= \frac{\partial L}{\partial \beta} \beta + \frac{\partial L}{\partial p} p + \frac{\partial L}{\partial r} r \\ C \frac{dr}{dt} - E \frac{dp}{dt} &= \frac{\partial N}{\partial \beta} \beta + \frac{\partial N}{\partial p} p + \frac{\partial N}{\partial r} r \end{aligned} \right\} \quad (8)$$

If equation (6) is differentiated together with equations (8), a system of three linear homogeneous differential equations is obtained because  $p = d\phi/dt$  and  $r = d\psi/dt$ .

$$\left. \begin{aligned} mV \left( -\frac{d^2\beta}{dt^2} + \frac{dr}{dt} \right) &= \frac{\partial Y}{\partial \beta} \frac{d\beta}{dt} + C_L \frac{\rho V^2}{2} S(p + r \tan \theta) \\ A \frac{dp}{dt} - E \frac{dr}{dt} &= \frac{\partial L}{\partial \beta} \beta + \frac{\partial L}{\partial p} p + \frac{\partial L}{\partial r} r \\ C \frac{dr}{dt} - E \frac{dp}{dt} &= \frac{\partial N}{\partial \beta} \beta + \frac{\partial N}{\partial p} p + \frac{\partial N}{\partial r} r \end{aligned} \right\} \quad (9)$$

Nondimensional magnitudes are now introduced by the equations

$$Y = C_y \frac{\rho V^2}{2} S^*$$

$$L = C_L \frac{\rho V^2}{2} S_b$$

$$N = C_n \frac{\rho V^2}{2} S_b$$

$$A = i_A \frac{mb^2}{4}$$

(10)

---

\*  $C_y$  is here the lateral force coefficient which should not be confused with the previously used notation for the lift coefficient.

$$C = i_C \frac{mb^2}{4}$$

$$E = i_E \frac{mb^2}{4}$$

$$\bar{p} = \frac{pb}{2V}$$

$$\bar{r} = \frac{rb}{2V}$$

$$\frac{\partial Y}{\partial \beta} = \frac{\partial C_Y}{\partial \beta} \frac{\rho V^2}{2} S = y_\beta \frac{\rho V^2}{2} S$$

$$y_\beta = \frac{\partial C_Y}{\partial \beta}$$

$$\frac{\partial L}{\partial \beta} = \frac{\partial C_L}{\partial \beta} \frac{\rho V^2}{2} S b = l_\beta \frac{\rho V^2}{2} S b$$

$$l_\beta = \frac{\partial C_L}{\partial \beta}$$

$$\frac{\partial N}{\partial \beta} = \frac{\partial C_n}{\partial \beta} \frac{\rho V^2}{2} S b = n_\beta \frac{\rho V^2}{2} S b$$

$$n_\beta = \frac{\partial C_n}{\partial \beta}$$

$$\frac{\partial L}{\partial p} p = \frac{\partial L}{\partial \frac{pb}{2V}} \frac{pb}{2V} = \bar{p} \frac{\partial C_L}{\partial \frac{pb}{2V}} \frac{\rho V^2}{2} S b = \bar{p} l_p \frac{\rho V^2}{2} S b$$

$$l_p = \frac{\partial C_L}{\partial \frac{pb}{2V}}$$

$$\frac{\partial L}{\partial r} r = \bar{r} l_r \frac{\rho V^2}{2} S b$$

$$l_r = \frac{\partial C_L}{\partial \frac{rb}{2V}}$$

$$\frac{\partial N}{\partial p} p = \bar{p} n_p \frac{\rho V^2}{2} S b$$

$$n_p = \frac{\partial C_n}{\partial \frac{pb}{2V}}$$

$$\frac{\partial N}{\partial r} r = \bar{r} n_r \frac{\rho V^2}{2} S b$$

$$n_r = \frac{\partial C_n}{\partial \frac{rb}{2V}}$$

If all terms on the left in equation (9) are transferred and the nondimensional magnitudes are introduced, the system becomes

$$mV \frac{d^2\beta}{dt^2} - mV \frac{2V}{b} \frac{d\bar{r}}{dt} + \frac{\rho V^2}{2} S y_{\beta} \frac{d\beta}{dt} + C_L \frac{\rho V^2}{2} S' \frac{2V}{b} (\bar{p} + \bar{r} \tan \theta) = 0$$

$$i_A \frac{mb^2}{4} \frac{2V}{b} \frac{d\bar{p}}{dt} - i_E \frac{mb^2}{4} \frac{2V}{b} \frac{d\bar{r}}{dt} - \frac{\rho V^2}{2} S b l_p \bar{p} - \frac{\rho V^2}{2} S b l_r \bar{r} - \frac{\rho V^2}{2} S b l_{\beta} \beta = 0$$

$$i_C \frac{mb^2}{4} \frac{2V}{b} \frac{d\bar{r}}{dt} - i_E \frac{mb^2}{4} \frac{2V}{b} \frac{d\bar{p}}{dt} - \frac{\rho V^2}{2} S b n_p \bar{p} - \frac{\rho V^2}{2} S b n_r \bar{r} - \frac{\rho V^2}{2} S b n_{\beta} \beta = 0$$

If the first equation of the system is divided by  $\rho^2 V^3 S^2 / m$ , the second by  $i_A \frac{\rho V^2 S b}{2}$ , and the third by  $i_C \frac{\rho V^2 S b}{2}$ , the following equations are obtained:

$$\left(\frac{m}{\rho S V}\right)^2 \frac{d^2\beta}{dt^2} + \frac{1}{2} y_{\beta} \frac{d\beta}{dt} \frac{m}{\rho S V} + \frac{C_L}{2} \frac{2m}{\rho S b} \bar{p} - \frac{2m}{\rho S b} \frac{m}{\rho S V} \frac{d\bar{r}}{dt} +$$

$$\frac{C_L}{2} \frac{2m}{\rho S b} \tan \theta X \bar{r} = 0$$

$$- \frac{l_{\beta}}{i_A} \beta + \frac{m}{\rho S V} \frac{d\bar{p}}{dt} - \frac{l_p}{i_A} \bar{p} - \frac{i_E}{i_A} \frac{m}{\rho S V} \frac{d\bar{r}}{dt} - \frac{l_r}{i_A} \bar{r} = 0$$

$$- \frac{n_{\beta}}{i_C} \beta - \frac{n_p}{i_C} \bar{p} - \frac{i_E}{i_C} \frac{m}{\rho S V} \frac{d\bar{p}}{dt} + \frac{m}{\rho S V} \frac{d\bar{r}}{dt} - \frac{n_r}{i_C} \bar{r} = 0$$

By setting

$$\tau = \frac{m}{\rho S V}$$

(11)

$$\mu = \frac{2m}{\rho S V}$$

and by introducing a nondimensional time by the equation

$$\bar{t} = \frac{t}{\tau}$$

(12)

Moreover, if the signs in the second and third equations are changed, the following system of equations in nondimensional form is obtained:

$$\left. \begin{aligned} \frac{d^2\bar{\beta}}{d\bar{t}^2} + \frac{1}{2} y_\beta \frac{d\bar{\beta}}{d\bar{t}} + \frac{C_L}{2} \bar{\mu} \bar{p} - \mu \frac{d\bar{r}}{d\bar{t}} + \frac{C_L}{2} \mu \tan \theta \bar{r} &= 0 \\ \frac{l_\beta}{i_A} \bar{\beta} - \frac{d\bar{p}}{d\bar{t}} + \frac{l_p}{i_A} \bar{p} + \frac{i_E}{i_A} \frac{d\bar{r}}{d\bar{t}} + \frac{l_r}{i_A} \bar{r} &= 0 \\ \frac{n_\beta}{i_C} \bar{\beta} + \frac{n_p}{i_C} \bar{p} + \frac{i_E}{i_C} \frac{d\bar{p}}{d\bar{t}} - \frac{d\bar{r}}{d\bar{t}} + \frac{n_r}{i_C} \bar{r} &= 0 \end{aligned} \right\} \quad (13)$$

The magnitudes  $y_\beta = \frac{\partial C_y}{\partial \beta}$ ,  $n_\beta = \frac{\partial C_n}{\partial \beta}$ , and  $l_\beta = \frac{\partial C_l}{\partial \beta}$  are determined from the usual tests in the wind tunnel and are denoted as the static derivatives. The magnitudes  $l_p$ ,  $l_r$ ,  $n_p$ , and  $n_r$  characterize the moments of the aerodynamic forces in rotation and for this reason they are known as the rotary derivatives.

## 2. THEORETICAL DETERMINATION OF DERIVATIVES OF LATERAL DYNAMIC STABILITY

As has been pointed out, all aerodynamic coefficients are referred to a system of axes: the X-axis is parallel to the velocity and passes through the center of gravity of the airplane at the initial instant; the Y-axis passes along the span of the wing to the right of the pilot; and the Z-axis is perpendicular to the first two and directed downward<sup>3</sup>. The positive direction of the angles of rotation and of the moments are assumed to be the following:

about the X-axis, motion from the Y-axis to the Z-axis  
 about the Y-axis, motion from the Z-axis to the X-axis  
 about the Z-axis, motion from the X-axis to the Y-axis

This system of axes is fixed in the airplane so that the X-axis coincides with the velocity of the airplane only at the initial

---

<sup>3</sup>This system of axes is in accordance with the terminology adopted by CAHI, May 1939.

2074

instant of time. For a disturbed motion of the airplane, the X-axis of the fixed system of axes makes an angle  $\beta$ , which is termed the sideslip angle, with the flight velocity.

The moments about the X- and Z-axis are denoted by L and N, respectively, and the angular velocities about the X- and Z-axis by p and r, respectively.

#### ROTARY DERIVATIVE $l_p$

In the following discussion, all the derivatives in the below-stall range will be considered. In the case of rotation of the airplane about the X-axis (angular velocity p), an aerodynamic damping moment arises about the same axis. This moment may be determined by the equation

$$L = \frac{pb}{2V} l_p \frac{\rho V^2}{2} S b$$

where

$l_p$  moment coefficient

$\frac{pb}{2V} = \bar{p}$  nondimensional velocity of roll

Here as usual (reference 1), a linear dependence of the aerodynamic reaction on the disturbance is assumed. The rolling moment is proportional to the fourth power of the linear dimension, and therefore the moment on the tail surface for an angular velocity  $\bar{p}$  is negligibly small as compared with the moment acting on the wing. Hence, in computing  $l_p$  only the moment acting on the wing shall be taken into consideration.

On rotation of the airplane about the longitudinal X-axis with angular velocity  $\bar{p} > 0$  (the right wing drops); at a flight velocity V, it is found that the angle of attack increases on the right wing. At the distance y from the plane of symmetry

$$\Delta\alpha \approx \tan \alpha = \frac{py}{V}$$

Similarly, on the left side of the wing the angle of attack decreases. A moment therefore appears opposing the rotation. Thus, for  $p > 0$ ,  $L < 0$ ; and the coefficient of the derivative of the rolling moment with respect to the angular velocity of roll is always (at below-stall angles of attack) negative (fig. 5)  $l_p < 0$ . Figure 6 gives curves by which  $l_p$  for wings of various aspect ratios and tapers may be determined (references 4 and 5).

Example:  $\eta = 1.94$ ,  $\lambda = 6.34$ .

From figure 6:  $l_p = -0.465$ .

It can be seen from the curves that  $l_p$  increases in absolute value with an increasing aspect ratio of the wings and that  $l_p$  decreases with increasing taper  $l_p$ .

The value of  $l_p$  is computed on the basis of the general theory of the wing with account taken of the change in the distribution of the circulation along the span due to rotation without considering the change in velocity along the span. At below-stalling angles, the derivative  $l_p$  theoretically does not depend on the initial twist of the wing nor on the angle of attack of the entire wing. The magnitude  $l_p$  varies little for different wings, as may be seen in figure 6. The mean value is  $l_p = -0.45$ . The sign of  $l_p$  may change only in the above-stalling range in the region of autorotation of the wing.

#### ROTARY DERIVATIVE $n_p$

In the rotation of the airplane about the X-axis, the angle of attack varies along the wing span and as a result the lift force and the induced drag will not be the same at symmetrical elements. Hence, when the airplane rotates about the X-axis, the airplane will be acted on by a moment of the aerodynamic forces both about the X-axis ( $l_p$ ) and about the Z-axis ( $n_p$ ). As before, consider that the moment about the Z-axis arising for angular velocity  $p$  is proportional to the angular velocity of rotation, so that

$$N = \frac{pb}{2V} n_p q S b$$

where  $q$  is the dynamic pressure.

The moment of yaw due to the angular velocity depends little on the tail surface so that in the computations for the dynamic stability only the moment due to the wing is taken into account.

For positive rotation in roll  $p > 0$  (right side of wing drops), the results show that on elements of the right and left wing the lift force vector  $L$  and the vector of induced drag  $D$  are rotated and changed (fig. 7). The airplane will therefore be acted on by a moment about the Z-axis (moment of yaw), which for negative angles may be positive and with increase in the angle of attack of the wing varies linearly so that at moderate angles of attack  $n_p$  is always negative ( $n_p < 0$  (fig. 7)). Curves of the values  $n_p/\alpha_a$  (reference 4) for untwisted wings<sup>4</sup> of various tapers and aspect ratios are shown in figure 8. The curves give the values of  $n_p/\alpha_a$  where  $\alpha_a$  is the angle of attack in degrees and is computed from the line of zero lift. Hence, in order to actually compute the value of  $n_p$ , it is necessary to multiply the value obtained from the curves for the given wing (given aspect ratio and taper) by the angle of attack (in degrees) computed from the line of zero lift.

For example,  $\eta = 1.94$ ,  $\lambda = 6.34$ ,  $\alpha_a = 9^\circ$  ( $\alpha_a$  is computed from the angle of zero lift). From figure 8,  $n_p/\alpha_a = -0.00395$  and, therefore,  $(n_p)\alpha = 9^\circ = -0.00395 \times 9 = -0.0356$ .

#### ROTARY DERIVATIVE $l_r$

For positive angular velocity  $r$ , the left wing moves forward, that is, the left wing has a greater velocity than the right wing. Therefore, the lift force on an element of the left wing will be greater than the lift force on the symmetrical element of the right wing and as a result the airplane will be acted on by an aerodynamic moment tending to lift the left wing, that is, a positive moment about the X-axis. With increase in the angular velocity  $r$ , the moment  $L$  increases in magnitude and the derivative of this moment with respect to the angular velocity  $\bar{r} = rb/2V$  will be positive (at positive  $C_L$ )<sup>5</sup>.

<sup>4</sup>The value of  $n_p$  little affects the characteristic of the dynamic stability and therefore a correction for the twist of the wing need not be introduced.

<sup>5</sup>Here, as previously, linear dependence of the moment on the angular velocity is assumed as is permissible because only small angular velocities are considered and the terms containing the squares of these velocities may be neglected.

$$L = \frac{rb}{2V} l_r q S b$$

$$l_r > 0$$

The coefficient  $l_r$  is determined for the wing and is proportional to the angle of attack  $\alpha_a$ . Evidently, both the wing taper and the aspect ratio will affect the value of  $l_r$ . Curves of the variation of  $l_r/\alpha_a$  for untwisted wings of various tapers and aspect ratios are given in figure 10. From the curves it may be seen that  $l_r$  decreases with increase in the taper and increases with increase in the aspect ratio.

It is also apparent in figure 10 that  $l_r/\alpha_a$  for various types of airplane changes little with wings of different tapers and aspect ratios. The mean value is  $l_r/\alpha_a = 0.017$   
0.018

In order to obtain the value of  $l_r$  at a given angle of attack, the value  $l_r/\alpha_a$  obtained from the curves must be multiplied by the angle of attack (in degrees) for which the computation is conducted (the angle of attack is measured from the line of zero lift).

For example,  $\eta = 1.94$ ,  $\lambda = 6.34$ ,  $\alpha_a = 9^\circ$ . From figure 10  $l_r/\alpha_a = 0.0185$ ;  $l_r = 0.0185 \times 9 = 0.1665$ . The vertical tail surface will also affect the derivative  $l_r$  of the airplane. The part of  $l_r$  due to the tail may be obtained from the equation

$$l_r = a_t K_t \left( \frac{l_t}{b} \right)^2 \frac{S_{tf}}{S} \sin 2(x - \alpha_a), \quad (14)$$

where

$$a_t = (\partial C_L / \partial \alpha)_t \quad (\text{fig. 11}).$$

$K_t$  empirical interference coefficient at tail, mean value = 0.8

$l_t$  distance from center of gravity of airplane to rudder hinge

$S_{tf}$	area of vertical tail surface with part of fuselage
$b$	wing span
$S$	wing area
$x$	angle between line of zero lift and line connecting center of gravity of airplane with geometric center of vertical tail surface (including part of fuselage) (for a low wing airplane $x > 0$ )
$\alpha_a$	angle of attack (from line of zero lift), degrees

Example:  $\alpha_t = 2.05$      $K_t = 0.8$      $\frac{l_t}{b} = 0.389$      $\frac{S_{tf}}{S} = 0.093$   
 $x = 12^\circ$

To find  $l_{rt}$  for  $\alpha_a = 9^\circ$ , from equation 14,

$$l_{rt} = 2.05 \times 0.8 (0.389)^2 \times 0.093 \times 0.105 = 0.00242$$

#### CORRECTION ON DERIVATIVE $l_r$ FOR TWIST OF WING

In order to introduce a correction for twist, it is necessary to use figure 12. Only the practical determination of the correction will be considered here<sup>6</sup>. The correction for twist for wings of various aspect ratios and the taper  $\eta = 3$  can be found by use of figure 12.

For a taper different from 3, the correction would be somewhat different but the error will be very small and it may therefore be assumed that the correction for twist does not depend on the wing taper. Assume, for example, the correction for the wing is found to be  $\lambda = 6.34$ , the twist of the wing starts at the distance  $0.226 b/2$  from the root, increases linearly, and at the tip attains the value  $1.5^\circ$ .

At the distance  $y = 0.226 b/2$  from the root, the twist is equal to zero (fig. 13(b)). In figure 13(a) at  $y = 0.226 b/2$ ,  $\Delta_1 = 0.001$ . Subtracting this value from  $D$  (fig. 13(a)), 0.0168 is

---

<sup>6</sup>This method and the curves are taken from reference 5, where a more detailed description of the curves is found.

obtained. This number is plotted in figure 13(c) and corresponds to an angle of twist equal to zero; therefore, on the curve of figure 13(c) the point (0, 0.0168) is plotted. It can be seen that at the distance  $0.4 b/2$  the angle of twist is  $0.3^\circ$  (fig. 13(b)) and from figure 13(a)  $\Delta_2 = 0.003$ ;  $l_r/\alpha = D - \Delta_2 = 0.0158$ . In figure 13(c)  $0.3^\circ$  is plotted as the abscissa and  $-0.0158$  as the ordinate, and so forth. A certain area is then obtained on the planimetry for which the correction in  $l_r$  is obtained.

For the given case,  $l_r \text{ twist} = 0.0144$ .

This correction does not depend on the angle of attack of the wing<sup>7</sup>.

For the total value of  $l_r$

$$l_r = \left(\frac{l_r}{\alpha_a}\right)\alpha_a + l_{rt} + l_r \text{ twist} \quad (15)$$

Example: find  $l_r$ :  $\lambda = 6.34$ ,  $\eta = 1.94$ ,  $\alpha_a = 9^\circ$ ,  $a_t = 2.05$ ,  
 $K_t = 0.8$ ,  $l_t/b = 0.389$ ,  $S_{tf}/S = 0.093$ ,  $x = 12^\circ$

The twist starts at  $0.226$  of the half span, increases linearly, and at the tip reaches the value  $1.5^\circ$

$$l_r = (l_r/\alpha_a)\alpha_a + l_{rt} + l_r \text{ twist} = 0.1665 + 0.00242 + 0.0144 = 0.1833$$

#### ROTARY DERIVATIVE $n_r$

During an angular velocity of rotation about the Z-axis (angular velocity of yaw  $r$ ) a yawing moment arises, which depends on the vertical tail surface, the fuselage, and the wing. At an angular velocity  $r$ , on account of the difference in the velocities at the symmetrical elements of the wing, different drags are obtained as a result of which there arises a moment about the Z-axis (moment of yaw  $N$ ). Evidently, the moment  $N$  due to the wing will be negative for positive values of  $r$  (fig. 14). Similarly, for the angular velocity  $r > 0$  a negative yawing moment is found to arise because of the fuselage and the tail.

---

<sup>7</sup>The value of  $l_r \text{ twist}$  is positive for the case where the angle of attack at the tip of the wing is greater than the angle of attack at the root section.

The yawing moment will increase in absolute value with increase in  $r$ ; hence,

$$N = \frac{rb}{2V} n_r q S b$$

$$n_r < 0 \text{ (fig. 14).}$$

The effect of the tail and the wing on the derivative  $n_r$  will now be considered.

#### Effect of Vertical Tail Surface on $n_r$

In the oscillation of the airplane about the Z-axis, that is, at an angular velocity  $r$ , the tail surface is found to be acted upon by the force

$$F = \left( \frac{dC_L}{d\alpha} \right)_t \frac{rl_t}{V} \frac{\rho S_{tF} V_t^2}{2} \cos(x - \alpha_a)$$

where  $x$  is the angle between the line of zero lift and the line connecting the center of gravity with the geometric center of the vertical tail surface with part of the fuselage. For a low-wing airplane, the angle  $x > 0$ . In the expression for the force during oscillations about the Z-axis there enters  $\cos(x - \alpha_a)$  because the system of axes is fixed. If the derivative of the moment of this force is taken about the center of gravity with respect to the non-dimensional angular velocity  $\bar{r} = rb/2V$ ,

$$N_{rt} = -2 \left( \frac{dC_L}{d\alpha} \right)_t \frac{l_t^2}{b} \frac{\rho S_{tF} V_t^2}{2} \cos^2(x - \alpha_a)$$

Finally, the nondimensional derivative  $n_r$  is obtained by dividing this expression by  $\rho S V^2 b/2$

$$n_{rt} = -2 \left( \frac{dC_L}{d\alpha} \right)_t \left( \frac{l_t}{b} \right)^2 \frac{S_{tF}}{S} \left( \frac{V_t}{V} \right)^2 \cos^2(x - \alpha_a)$$

In this equation no account is taken of the effect of the fuselage on the flow at the vertical tail surface. The indeterminacy of the magnitude of the interference at the vertical tail surface makes the theoretical computation of the moments due to the vertical tail

surface inaccurate. An empirical coefficient  $K_t$  characterizing the velocity interference at the tail surface is therefore introduced. Moreover, setting

$$\left(\frac{dC_l}{d\alpha}\right)_t = a_t$$

gives

$$n_{rt} = -2K_t a_t \left(\frac{l_t}{b}\right)^2 \frac{S_{tf}}{S} \cos^2(x - \alpha_a)$$

By permitting a small error, it may be assumed that  $\cos^2(x - \alpha_a) \approx 1$  and then

$$n_{rt} = -2K_t a_t \left(\frac{l_t}{b}\right)^2 \frac{S_{tf}}{S} \tag{16}$$

where

- $l_t$  distance from center of gravity of airplane to rudder hinge
- $b$  wing span
- $S_{tf}$  area of vertical tail surface with part of fuselage
- $S$  area of wing

For the coefficient  $K_t$ , the value 0.8 may be taken.

The value of  $a_t$  depends on the aspect ratio of the vertical tail surface.

Figure 11 shows the dependence of  $a_t$  on the experimentally obtained aspect ratio  $\lambda_t$  (reference 6). The mean value of the coefficient  $a_t$  for airplanes of the usual type is

$$a_t = 2.2$$

In order to compute the aspect ratio of the vertical tail surface  $\lambda_t$ , the span of the tail  $b_t$  must be taken as shown in figure 11. In the tail surface area  $S_{tf}$  there is included the end of the

207A

fuselage (hatched area in fig. 11). The effect of the fuselage is not taken into account in equation (16). In the same manner as for determining the damping of longitudinal oscillations, the coefficient 1.25 in equation (16) is introduced to take account of the fuselage. Then

$$n_{rtf} = 2.5K + a_t \left( \frac{l_t}{b} \right)^2 \frac{S_{tf}}{S} \quad (16a)$$

Example:  $K_t = 0.8$        $a_t = 2.05$   
 $l_t/b = 0.389$        $S_{tf}/S = 0.093$

By formula (16a),

$$n_{rtf} = 2.5 \times 0.8 \times 2.05 \times (0.389)^2 \times 0.093 = -0.0577$$

#### Effect of Wing on Derivative $n_r$

For positive angular velocity about the Z-axis ( $r > 0$ ), the velocity on the left wing increases and on the right decreases. Hence, the drag on the left wing will be greater than on the right wing and there appears a moment about the Z-axis acting against the rotation (fig. 14).

The damping moment of  $n_r$  from the wing is due to the induced and profile drags.

Curves for the determination of  $n_r$  of the wing due to the induced drag are given in figure 15. In order to determine  $n_r$  from figure 15, it is necessary to multiply the value of  $n_r/\alpha_a^2$  by  $\alpha_a^2$  where  $\alpha_a$  is the angle of attack of the wing computed from the line of zero lift in degrees. The part  $n_r$  of the wing, which is obtained as the result of the profile drag, is small and need not be taken into account<sup>8</sup>.

---

<sup>8</sup>The curves for computing this part of the derivative  $n_r$  are given in reference 5.

Example. Find  $n_r$  of the wing:  $\eta = 1.94$ ,  $\lambda = 6.34$ ,  $\alpha_a = 9^\circ$ .

In figure 15,  $n_r/\alpha_a^2 = -0.000147$ ,  $n_{rw} = -0.000147 \times 9^2 = -0.0119$ .

The total value of the derivative  $n_r$  for the airplane may be obtained from the formula

$$n_r = n_{rtf} + n_{rw} \quad (16b)$$

Example: Find  $n_r$  of the airplane  $\alpha_a = 9^\circ$ .

The characteristics of the wing are:  $\eta = 1.94$  and  $\lambda = 6.34$ .

The characteristics of the tail surface are  $St_f/S = 0.093$ ,  $l_t/b = 0.389$ ,  $\lambda_t = 1.14$ .

$$n_r = n_{rtf} + n_{rw} = -0.0577 - 0.0119 = -0.0696$$

It must be borne in mind that at times the interference of the fuselage has a strong effect on  $n_r$ . For example, for one model a value of  $n_r$  of the tail and the fuselage was obtained equal to a third of the derivative  $n_r$  for the tail only. Hence, a sufficiently reliable determination of  $n_r$  can be obtained only by experiment. The theoretical equations for determining  $n_r$  may in individual cases give considerable error and should be considered only as rough approximations<sup>9</sup>.

Equations have been derived herein for the computation of the rotary derivatives, that is, the coefficients of the moments obtained during rotational motion of the airplane (yaw or roll). The determination of the coefficients of the forces and the moment of the aerodynamic forces in sideslip follows. These coefficients are called static derivatives.

---

<sup>9</sup>Early in 1940 at CAHI, work will be completed on the determination of the derivative  $n_r$  for 10 to 15 models. From this investigation, the value of the derivative  $n_r$  can be obtained for similar airplanes.

DETERMINATION OF STATIC DERIVATIVE  $l_\beta$ 

For a positive sideslip angle  $\beta$  the left wing moves forward, the flow under the left wing tending to lift it, that is, for  $\beta > 0$  the rolling moment  $L$  is positive and

$$L = L_\beta \beta = \beta l_\beta q S b > 0$$

$$l_\beta > 0 \text{ (fig. 16)}$$

Experiment shows the static derivative  $l_\beta$  may be found by the formula

$$l_\beta \text{ airp} = (l_\beta)_{\psi=0} + \psi \frac{\partial l_\beta}{\partial \psi} + \chi \frac{\partial l_\beta}{\partial \chi} + l_\beta \text{ fus} + l_\beta \text{t} \quad (17)$$

$\chi = 0$

where

$\psi$  angle of dihedral of wing

$\chi$  sweepback angle of the wing

The characteristics of the individual terms in the equation will now be discussed. The magnitude  $(l_\beta)_{\psi=0}$  gives  $l_\beta$  for the

wing in the absence of sweepback and dihedral. The derivative  $(l_\beta)_{\psi=0}$  arises from the change in distribution of the circulation

over the wing span as the result of the sideslip. Test curves show that this derivative increases with increasing angle of attack.

This magnitude cannot be computed on account of the absence of test data. The plan form of the wing considerably affects the value of this coefficient. A rectangular wing without rounded tips gives a value much greater than a wing with rounded tips (reference 7).

The effect of the dihedral of the wing is taken care of by the term  $\psi \frac{\partial l_\beta}{\partial \psi}$ . The angle of wing dihedral  $\psi$  is measured between the plane of the chords and the plane perpendicular to the plane of symmetry of the airplane and passing through the root chord (fig. 17).

Experiment shows that  $l_\beta$  is proportional to the dihedral  $\psi$  with a coefficient of proportionality  $\partial l_\beta / \partial \psi$ , which may be determined from figure 18, which gives the values of the derivate  $l_\beta$  for a wing without a straight midwing section.

Example: Find  $l_\beta$  of the wing:  $\eta = 1.94$ ,  $\lambda = 6.34$ ,  $\psi = 4.25^\circ$ .

According to figure 18,  $\partial l_\beta / \partial \psi = 0.0133$ .

$$l_\beta = \psi \frac{\partial l_\beta}{\partial \psi} = 4.25 \times 0.0133 = 0.0565$$

For a wing with a midwing section it is necessary to subtract from the value obtained from figure 18 the amount

$$\left( \frac{\partial l_\beta}{\partial \psi} \right)_{mw} = 0.02 \left( \frac{b_{mw}}{b} \right)^2 \quad (18)$$

where  $b_{mw}/b$  is the ratio of the span of the midwing section to the span of the wing. The angle  $\psi$  in this case is to be measured as shown in figure 17(b).

Example:  $\eta = 1.94$ ,  $\lambda = 6.34$ ,  $\psi = 4.25^\circ$ ,  $b_{mw}/b = 0.226$

$$l_\beta = 4.25 \left[ 0.0133 - 0.02(0.226)^2 \right] = 0.0523.$$

Tests show that the tip of the wing greatly affects the value of the derivative  $l_\beta$ . The wing tip in vertical projection may be such as shown in figure 19.

From specially conducted tests (reference 7), it was found that if the wing tip is of the shape shown in figure 19(c), the effective dihedral is increased by 1 to 1.5°.

#### Effect of Sweepback

The angle of sweepback is measured between the lines passing through the focal line at 0.25 chord from the leading edge of the wing and the plane perpendicular to the axis of the fuselage. The sweepback angle  $\chi$  will be considered positive for the direction

shown in figure 20. For a positive sweepback at a positive sideslip angle, the flow about the left wing is improved and the lift force on the left wing is increased. As a result, an increase in the rolling moment is obtained for positive sweepback

$$\chi > 0, \ell_{\beta} > 0$$

The effect of sweepback is taken into account in equation (17) by the term  $\chi \frac{\partial \ell_{\beta}}{\partial \chi}$ . At the present time sufficient data, by use of which the effect of the sweepback for different wings could be determined, are unavailable. F. Weick (reference 8) recommends for rectilinear wings of aspect ratio 6 the equation

$$\frac{\partial \ell_{\beta}}{\partial \chi} = 0.0045 C_L \quad (19)$$

where  $\chi$  is the sweepback angle in degrees.

Example.  $\chi = 2.5^\circ$ ,  $C_L = 0.73$  ( $\alpha = 9^\circ$ )

From equation (19)

$$\ell_{\beta} = \chi \frac{\partial \ell_{\beta}}{\partial \chi} = 2.5(0.0045 \times 0.73) = 0.00822$$

#### Effect of Position of Wing Relative to Fuselage

The previously described relations give  $\ell_{\beta}$  for isolated wings. Tests show, however, a very great effect of the position of the wing with respect to the fuselage on the derivative  $\ell_{\beta}$ . It was found, for example, that a center wing gives a value for  $\ell_{\beta}$  approximately agreeing with the value for the isolated wing. A high wing increases the effective dihedral by  $1^\circ$  to  $1.5^\circ$  and a low wing decreases the effective dihedral by  $2^\circ$  to  $5^\circ$ . This change in the effective dihedral occurs, however, at small and medium angles of attack. At large angles of attack different results may be obtained, which at the present time, due to the absence of sufficient test data, cannot be even approximately predicted.

On account of the resistance of the flow, all projections at the lower surface of the wing increase  $\ell_{\beta}$  and conversely all projections on the upper surface decrease  $\ell_{\beta}$ . In a fixed system of

12074

axes, the X-axis passes below the center of pressure of the vertical tail surface; therefore, the vertical tail surface will also give a rolling moment in sideslip. If the angle between the line connecting the center of gravity with the center of pressure of the vertical tail surface and the velocity is denoted by  $\alpha_a - x$

$$l_{\beta t} = K_t a_t \frac{l_t}{b} \frac{S_{tf}}{S} \sin(x - \alpha_a) \quad (20)$$

Example.  $K_t = 0.8$ ,  $l_t/b = 0.389$ ,  $S_{tf}/S = 0.093$ ,  $a_t = 2.05$ ,  $x = 12^\circ$ ,  
 $\alpha_a = 9^\circ$

By equation 20

$$l_{\beta t} = 0.8 \times 0.389 \times 0.093 \times 2.05 \times 0.0523 = 0.00597$$

It follows from the foregoing discussion that the derivative  $l_{\beta}$  may be determined with sufficient accuracy only by experiment. These equations for determining the effect of the dihedral and sweepback of the wing may be used for estimating the changes in the airplane parameters after tunnel tests. For example, if from computation of the test data it is found that it is necessary to increase  $l_{\beta}$  by 0.026 and the parameters of the wing are  $\eta = 3$ ,  $\lambda = 7$  (without mid wing) the required increase in the dihedral  $\Delta\psi$  is obtained from the relation  $\Delta\psi \times 0.0133 = 0.026$  (the value 0.0133 is obtained from fig. 18) whence  $\Delta\psi = 2^\circ$ . If in another case it is necessary (for example, from considerations of longitudinal stability) to decrease the sweepback by  $\chi = 5^\circ$ , the change in  $l_{\beta}$  can be found. (The computation is conducted for the initial state of flight of the given airplane). Let  $C_L = 0.6$

$$\frac{\partial l_{\beta}}{\partial \chi} = 0.0045 C_L = 0.0045 \times 0.6 = 0.0027$$

$$\Delta l_{\beta} = 0.0027 \times 5 = 0.0135$$

Hence, decreasing the dihedral by  $5^\circ$ ,  $l_{\beta}$  decreases by  $\Delta l_{\beta} = 0.0135$ . In order to compensate for the decrease in  $l_{\beta}$  the dihedral of the wing must be increased

$$\Delta\psi \times 0.0133 = 0.0135$$

whence

$$\Delta\psi = 1^\circ$$

that is, the dihedral must be increased by  $1^\circ$ .

#### DETERMINATION OF STATIC DERIVATIVE $n_\beta$

The static derivative  $n_\beta = \partial C_n / \partial \beta$  characterizes the change in the moment of yaw with change in the sideslip angle and depends mainly on the area and the shape of the vertical tail surface and the fuselage. The center of pressure of the fuselage for the usual arrangement is located ahead of the center of gravity and for this reason the yawing moment due to the fuselage for  $\beta > 0$  is positive, that is, the fuselage is unstable. As may be seen from figure 21,  $n_\beta < 0$ .

The magnitude of the coefficient  $n_\beta$  is determined analytically by the equation

$$n_\beta = n_{\beta f} + n_{\beta t} = K \frac{S_f}{S} \frac{l_f}{b} - K_t a_t \frac{l_t}{b} \frac{S_{tf}}{S} \quad (21)$$

where

$S_f$  lateral area of fuselage

$l_f$  length of fuselage

The coefficient  $K_\beta$  may be found from figure 22 (taken from reference 9)

where

$l_f$  length of fuselage (positive)

$l_{nf}$  distance of center of gravity from nose of airplane (positive)

$h$  maximum height of fuselage (positive)

The coefficient  $K_\beta$  ( $K_\beta > 0$ ) may be determined if the ratios  $l_f/h$  and  $l_{nf}/l_f$  are known.

2074

Example:  $l_f/h = 6.0$ ,  $l_{nf}/l_f = 0.244$

From figure 22 it can be seen that  $K_\beta = 0.106$ .

If  $S_f/S = 0.35$  and  $l_f/b = 0.595$  then  
 $n_{\beta f} = 0.106 \times 0.35 \times 0.595 = 0.0221$ . Equation (26) is suitable for airplanes with unstable fuselages. Sometimes the fuselage is stable (as is rarely the case) and this equation cannot then be applied. The value of  $a_t$  may be obtained from figure 11. The mean value for  $K_t$  is 0.8.

Example:  $l_t/b = 0.389$ ,  $S_{tf}/S = 0.093$ ,  $\lambda_t = 1.14$ .

From figure 11,  $a_t = 2.05$

$$n_{\beta t} = -0.8 \times 0.389 \times 0.093 \times 2.05 = -0.0593$$

$$n_\beta = n_{\beta f} + n_{\beta t} = 0.0221 - 0.0593 = -0.0372$$

Let the area of the tail surface be increased such that  $\Delta S_{tf}/S = 0.04$ . Then for the increase in the coefficient  $n_\beta$

$$\Delta n_\beta = -0.8 \times 0.389 \times 0.04 \times 2.05 = -0.0268$$

Thus, when it is required to increase the vertical tail area, the span must be increased but not the chord. If the vertical tail surface is increased by increasing the chord,  $\lambda_t$  decreases and therefore  $a_t$  also decreases; as a result for such an increase in  $S_{tf}$  the weathercock stability ( $n_\beta$ ) is found to undergo only slight increases or does not change at all.

The equations for determining the value of  $n_\beta$  must be considered to be only approximate. For a more accurate determination of  $n_\beta$ , recourse must be made to experiment. As in the case of determining the derivative  $l_\beta$ , these approximate equations may be used for computing the derivative  $n_\beta$  after the tail area is increased or decreased.

### Effect of Propeller

In the present investigation, the effect of the propeller slipstream on the dynamic-stability derivatives is not considered. The derivatives  $n_\beta$  and  $n_r$  evidently will be greatly affected by the propeller slipstream. Up to the present time, however, sufficiently accurate test data, by which a correction for the effect of the propeller on the tail surface may be introduced, are unavailable.

#### DETERMINATION OF STATIC DERIVATIVE $y_\beta$

The static derivative  $y_\beta$  (fig. 23) is always positive ( $y_\beta > 0$ ). The derivative  $y_\beta$  characterizes the increase in the lateral force ( $y$ ) acting on the airplane during an increase in the sideslip angle ( $\beta$ ). Evidently, the value of  $y_\beta$  depends essentially on the size and shape of the fuselage and of the vertical tail surface. Diehl (reference 10) recommends the following empirical equation for computing the derivative  $y_\beta$ :

$$y_\beta = 0.12 \frac{bl_f}{S} \quad (22)$$

Example:  $b = 14.53$ ,  $l_f = 8.67$ ,  $S = 33.4$

$$y_\beta = 0.12 \frac{bl_f}{S} = 0.12 \frac{14.53 \times 8.67}{33.4} = 0.453$$

For airplanes with usual fuselages, the mean value of  $y_\beta$  is 0.4; therefore, the derivative  $y_\beta$  has little effect on the characteristics of dynamic stability.

### 3. EXPERIMENTAL DETERMINATION OF DYNAMIC-STABILITY

#### DERIVATIVES

The dynamic-stability derivatives are divided into two groups; namely, the derivatives of the moments and forces with respect to the angular velocity, which are called the rotary derivatives, and the derivatives of the moments and forces with respect to the sideslip angle, which are the static derivatives.

The rotary derivatives may be determined in a wind tunnel on special apparatus. The procedure of these tests is, however, rather complicated and they will not be considered herein (reference 11).

The static derivatives  $n_\beta$ ,  $l_\beta$ , and  $y_\beta$  may be readily obtained from the results of the usual tests in the wind tunnel. For this purpose it is necessary to have the coefficients of yaw and roll and the lateral force ( $C_n$ ,  $C_l$ , and  $C_y$ ) for various angles  $\beta$  at the given angle of attack. Curves are given in figures 24 to 26 for the change in the coefficients  $C_n$ ,  $C_l$ , and  $C_y$  with sideslip angle.

If these coefficients are given in the fixed system of axes assumed at CAHI (fig. 1), then in determining the derivative  $n_\beta$ , the tangent to the curve  $C_n = f(\beta)$  for  $\beta = 0$  must be drawn and the slope of the angle of inclination measured (taking account of the scale). Special attention must be paid to the determination of the slope of the curve  $C_n = f(\beta)$ . The slope of this curve characterizes the weathercock stability. For stable airplanes, the curve is like that shown in figure 24, that is, the coefficient  $C_n$  decreases with increase in the sideslip angle  $\beta$ . For neutral or laterally unstable airplanes, the curves differ to a marked degree from those in figure 24 near  $\beta = 0$  only, in the range from  $\beta = -3^\circ$  to  $\beta = +3^\circ$ , where for neutral airplanes these curves run parallel to the axis of abscissas and for unstable airplanes the slope of the curve changes sign, that is, the coefficient  $C_n$  in this range increases with increase in  $\beta$ . For a sideslip angle less than  $B = -3^\circ$  or greater than  $B = +3^\circ$ , the curves in all cases are as shown in figures 24, that is, the coefficient  $C_n$  decreases with increase in the sideslip angle  $\beta$ . Hence, in determining the weathercock stability, the points lying within the range  $\beta = \pm 3^\circ$  must be considered. During the tests, points must be taken every  $1^\circ$  angle near  $\beta = 0$  but beyond  $|\beta| = 3^\circ$  points may be taken every  $2^\circ$  to  $3^\circ$ . The computations required for obtaining the derivative are presented in figures 24 to 26. The coefficient 57.3 is introduced into the computation for converting degrees into radians in measuring the angle  $\beta$ . For a sufficiently accurate determination of the derivatives  $n_\beta$ ,  $l_\beta$ , and  $y_\beta$ , it is necessary to compute them for  $4^\circ$  or  $5^\circ$  angles of attack. (See appendix 1.)

### Determination of Moments of Inertia of Airplane

In order to compute the lateral dynamic stability of the airplane, the coefficients of the moments of inertia, which can be obtained from the following formulas, must be known:

$$i_A = \frac{4A}{mb^2} \quad \text{and} \quad i_C = \frac{4C}{mb^2}$$

where

A polar moment of inertia with respect to X-axis

C polar moment of inertia with respect to Z-axis

b wing span

m mass of airplane

Because for various conditions of flight of the airplane (different angles of attack  $\alpha$ ) the axes X and Z rotate with respect to the airplane, it is evident that the moments of inertia will vary likewise. If the moments of inertia of the airplane about the principal axes (A' and C') are known, the moments of inertia about the X- and Z-axes may be computed by the following equations:

$$A = A' \cos^2 \varphi + C' \sin^2 \varphi, \quad C = C' \cos^2 \varphi + A' \sin^2 \varphi, \quad E = \frac{A' - C'}{2} \sin 2\varphi$$

(23)

Computations show that up to angles of attack  $\alpha = 15^\circ$  to  $20^\circ$  it may be assumed with a sufficient degree of accuracy that  $A = A'$  and  $C = C'$ , that is, the moments of inertia about the X- and Z-axes are equal to the corresponding moments of inertia about the principal axes. As will be shown, the centrifugal moment of inertia has little effect on the stability characteristics and therefore E need not be computed.

At the present time no sufficiently accurate statistical formulas exist by which the moments of inertia of an airplane may be quickly determined and it is therefore necessary to resort to analytical computation in each case. Formulas and the computing procedure of the moments of inertia are given in reference 12.

The values of  $i_A$  and  $i_C$  change within the ranges  
 $0.049 < i_A < 0.089$  and  $0.09 < i_C < 0.154$ .

#### Determination of "Airplane Density" $\mu$

The "airplane density"  $\mu$  is determined by formula (11)

$$\mu = \frac{2m}{cSb} = \frac{2 \frac{G}{S}}{\gamma b}$$

where

$G/S$  load/sq meter, ( $\text{kg}/\text{m}^2$ )

$\gamma$  unit weight of air

$b$  span, meters

The computation of the dynamic stability is usually conducted for the altitude  $H = 3000$  meters and therefore  $\gamma = 0.908$  kilograms per cubic meter. For the altitude  $H = 3000$  meters for standard atmosphere

$$\mu = 2.20 \frac{G/S}{b} \quad (24)$$

Example:

$$\frac{G}{S} = 78 \text{ kilograms per square meter}$$

$$b = 14.53 \text{ meters}$$

$$\mu = 2.2 \frac{78}{14.53} = 11.8$$

$\mu$  is a nondimensional magnitude.

Determination of  $\tau$ 

The magnitude  $\tau$  is determined by equation (11)

$$\tau = \frac{m}{\rho S V}$$

In determining  $\mu$  for  $H = 3000$  meters

$$\tau = 1.1 \frac{G}{S V} \quad (25)$$

where  $G/S$  is in kilograms per square meter,  $V$  is in meters per second, and  $\tau$  is in seconds.

Example:  $G/S = 78$  kilograms per square meter and  $V = 47.4$  meters per second

$$\tau = 1.1 \frac{G}{S V} = 1.1 \frac{78}{47.4} = 1.79 \text{ sec.}$$

## 4. SOLUTION OF SYSTEM OF EQUATIONS OF MOTION

A solution of the system of equations (13) will now be sought in the form

$$\beta = B e^{\lambda \bar{t}}; \quad \bar{p} = P e^{\lambda \bar{t}} \quad \text{and} \quad \bar{r} = R e^{\lambda \bar{t}}$$

By substituting in equations (13) and dividing by  $e^{\lambda \bar{t}}$ , the following equations are obtained:

$$\left( \lambda^2 + \frac{1}{2} y_{\beta} \lambda \right) B + \mu \frac{C_L}{2} P + \mu \left( \frac{C_L}{2} \tan \theta - \lambda \right) R = 0$$

$$\left( \frac{l_{\beta}}{i_A} \right) B - \left( \lambda - \frac{l_P}{i_A} \right) P + \left( \frac{i_E}{i_A} \lambda + \frac{l_R}{i_A} \right) R = 0$$

$$\frac{n_{\beta}}{i_C} B + \left( \frac{n_D}{i_C} + \frac{i_E}{i_C} \lambda \right) P - \left( \lambda - \frac{n_R}{i_C} \right) R = 0$$

The system of linear homogeneous equations has a solution if the determinant of the system is equal to zero.

$$\begin{vmatrix} \lambda^2 + \frac{1}{2} y_{\beta} \lambda & \mu \frac{C_L}{2} & \mu \left( \frac{C_L}{2} \tan \theta - \lambda \right) \\ \frac{z_{\beta}}{i_A} & -\lambda + \frac{z_P}{i_A} & \frac{i_E}{i_A} \lambda + \frac{z_r}{i_A} \\ \frac{n_{\beta}}{i_C} & \frac{n_P}{i_C} + \frac{i_E}{i_C} \lambda & -\lambda + \frac{n_r}{i_C} \end{vmatrix} = 0$$

In expanding the determinant, an equation of the fourth degree in  $\lambda$  is obtained, which is called the characteristic equation.

$$A_4 \lambda^4 + A_3 \lambda^3 + A_2 \lambda^2 + A_1 \lambda + A_0 = 0 \quad (26)$$

where

$$A_4 = 1 - \left( \frac{i_E}{i_A} \right) \left( \frac{i_E}{i_C} \right)$$

$$A_3 = \left( \frac{1}{2} y_{\beta} \right) \left[ 1 - \left( \frac{i_E}{i_A} \right) \left( \frac{i_E}{i_C} \right) \right] - \left[ \left( \frac{z_P}{i_A} \right) + \left( \frac{n_r}{i_C} \right) \right] - \left[ \frac{i_E}{i_A} \frac{n_P}{i_C} + \frac{i_E}{i_C} \frac{z_r}{i_A} \right]$$

$$A_2 = \frac{z_P}{i_A} \frac{n_r}{i_C} - \frac{n_P}{i_C} \frac{z_r}{i_A} - \left[ \frac{1}{2} y_{\beta} \right] \left[ \frac{z_P}{i_A} + \frac{n_r}{i_C} \right] -$$

$$\left[ \frac{1}{2} y_{\beta} \right] \left[ \frac{i_E}{i_C} \frac{z_r}{i_A} + \frac{i_E}{i_A} \frac{n_P}{i_C} \right] - \left[ \mu \frac{z_{\beta}}{i_A} \frac{i_E}{i_C} + \mu \frac{n_{\beta}}{i_C} \right]$$

$$A_1 = \left( \frac{1}{2} y_{\beta} \right) \left[ \frac{z_P}{i_A} \frac{n_r}{i_C} - \frac{n_P}{i_C} \frac{z_r}{i_A} \right] + \mu \frac{n_{\beta}}{i_C} \frac{z_P}{i_A} - \mu \frac{z_{\beta}}{i_A} \frac{n_P}{i_C} +$$

$$\frac{C_L}{2} \mu \frac{z_{\beta}}{i_A} \left( 1 + \frac{i_E}{z_C} \tan \theta \right) + \frac{C_L}{2} \mu \frac{n_{\beta}}{i_C} \left( \tan \theta + \frac{i_E}{i_A} \right)$$

$$A_0 = \mu \frac{C_L}{2} \left( \frac{z_r}{i_A} \frac{n_{\beta}}{i_C} - \frac{z_{\beta}}{i_A} \frac{n_r}{i_C} \right) + \mu \frac{C_L}{2} \tan \theta \left( \frac{n_P}{i_C} \frac{z_{\beta}}{i_A} - \frac{z_P}{i_A} \frac{n_{\beta}}{i_C} \right)$$

Analysis of the coefficients shows that up to angles of attack from  $15^\circ$  to  $20^\circ$  the magnitude  $i_E$  has little effect on the roots of the characteristic equation and without large error  $i_E = 0$ .

If in addition, this analysis is restricted to the consideration of level flight, that is,  $\tan \theta = 0$ , the following equation is obtained:

$$\begin{aligned}
 A_4 &= 1 \\
 A_3 &= \left( \frac{1}{2} y_\beta \right) - \left[ \frac{l_p}{i_A} + \frac{n_r}{i_C} \right] \\
 A_2 &= \left\{ \frac{l_p}{i_A} \frac{n_r}{i_C} - \frac{n_p}{i_C} \frac{l_r}{i_A} \right\} - \left( \frac{1}{2} y_\beta \right) \left[ \frac{l_p}{i_A} + \frac{n_r}{i_C} \right] - \mu \frac{n_\beta}{i_C} \\
 A_1 &= \left( \frac{1}{2} y_\beta \right) \left\{ \frac{l_p}{i_A} \frac{n_r}{i_C} - \frac{n_p}{i_C} \frac{l_r}{i_A} \right\} + \mu \frac{n_\beta}{i_C} \frac{l_p}{i_A} - \mu \frac{l_\beta}{i_A} \frac{n_p}{i_C} + \mu \frac{C_L}{2} \frac{l_\beta}{i_A} \\
 A_0 &= \mu \frac{C_L}{2} \left( \frac{l_r}{i_A} \frac{n_\beta}{i_C} - \frac{l_\beta}{i_A} \frac{n_r}{i_C} \right)
 \end{aligned} \tag{27}$$

Because

$$\begin{aligned}
 y_\beta &> 0, \quad l_\beta > 0, \quad n_\beta < 0 \\
 l_p &< 0, \quad l_r > 0, \quad n_p < 0, \quad n_r < 0, \quad C_L > 0 \\
 \mu &> 0, \quad i_A > 0, \quad i_C > 0
 \end{aligned}$$

The following relation is usually true:

$$A_3 > 0, \quad A_2 > 0, \quad A_1 > 0$$

The coefficient  $A_0$ , the free term of the characteristic equation, may be either positive or negative.

Example:

$$\frac{1}{2} y_{\beta} = 0.24; \quad \frac{l_{\beta}}{i_A} = 1.175; \quad \frac{n_{\beta}}{i_C} = -0.312$$

$$\frac{l_p}{i_A} = -7.27; \quad \frac{l_r}{i_A} = 3.11$$

$$\frac{n_p}{i_C} = -0.52; \quad \frac{n_r}{i_C} = -0.76$$

$$\frac{C_L}{2} = 0.37; \quad \mu = 11.8$$

In order to find the coefficients of the characteristic equation, use is made of equations (27):

$$A_3 = \frac{1}{2} y_{\beta} - \left[ \frac{l_p}{i_A} + \frac{n_r}{i_C} \right] = 0.24 - [-7.27 - 0.76] = 8.27$$

$$A_2 = \left\{ \frac{l_p}{i_A} \frac{n_r}{i_C} - \frac{n_p}{i_C} \frac{l_r}{i_A} \right\} - \left( \frac{1}{2} y_{\beta} \right) \left[ \frac{l_p}{i_A} + \frac{n_r}{i_C} \right] - \mu \frac{n_{\beta}}{i_C}$$

$$= \{7.27 \times 0.76 + 0.52 \times 3.11\} - 0.24 [-8.03] + 11.8 \times 0.312 = 12.7526$$

$$A_1 = \left( \frac{1}{2} y_{\beta} \right) \left\{ \frac{l_p}{i_A} \frac{n_r}{i_C} - \frac{n_p}{i_C} \frac{l_r}{i_A} \right\} + \mu \frac{n_{\beta}}{i_C} \frac{l_p}{i_A} - \mu \frac{l_{\beta}}{i_A} \frac{n_p}{i_C} + \mu \frac{C_L}{2} \frac{l_{\beta}}{i_A}$$

$$= 0.24 \{7.145\} + 11.8 \times 0.312 \times 7.27 + 11.8 \times 1.175 \times 0.52 +$$

$$11.8 \times 0.37 \times 1.175 = 40.809$$

$$A_0 = \mu \frac{C_L}{2} \left( \frac{l_r}{i_A} \frac{n_{\beta}}{i_C} - \frac{l_{\beta}}{i_A} \frac{n_r}{i_C} \right) = 11.8 \times 0.37 (-3.11 \times 0.312 +$$

$$1.175 \times 0.76) = -0.3362$$

If the roots of equation (26) are denoted by  $\lambda_1, \lambda_2, \lambda_3$ , and  $\lambda_4$ , the solution of the system (13) is obtained in the form

$$\beta = B_1 e^{\lambda_1 \bar{t}} + B_2 e^{\lambda_2 \bar{t}} + B_3 e^{\lambda_3 \bar{t}} + B_4 e^{\lambda_4 \bar{t}}$$

$$\bar{p} = P_1 e^{\lambda_1 \bar{t}} + P_2 e^{\lambda_2 \bar{t}} + P_3 e^{\lambda_3 \bar{t}} + P_4 e^{\lambda_4 \bar{t}}$$

$$\bar{r} = R_1 e^{\lambda_1 \bar{t}} + R_2 e^{\lambda_2 \bar{t}} + R_3 e^{\lambda_3 \bar{t}} + R_4 e^{\lambda_4 \bar{t}}$$

Evidently, in order that the sideslip angle and the angular velocities of the airplane  $\beta$ ,  $\bar{p}$ , and  $\bar{r}$  should decrease with time (that is, in order that the airplane should be dynamically stable), it is necessary that all real roots be negative and that the complex roots have negative real parts. In the general case, the solution of an algebraic equation of the fourth degree is laborious. In the given case, however, by making use of the special characteristics of the equation of lateral stability, this equation may be quickly and simply solved. The determination of the roots of equation (26) takes no more than 20 minutes.

For airplanes of the usual type, the characteristic equation of the lateral stability has two real roots of which one is very large and the other very small and two complex conjugate roots. The small real root is denoted by  $\lambda_1$ , the large real root by  $\lambda_2$ , and the complex conjugate roots by  $\lambda_3$  and  $\lambda_4$ . Because  $\lambda_1$  is very small, the following equation may be written with a large degree of accuracy:

$$A_1 \lambda + A_0 = 0$$

from which  $\lambda_1$  is immediately determined<sup>10</sup>.

---

<sup>10</sup>Practical computation shows that the value  $\lambda_1 = -A_0/A_1$  is accurate. For example, if  $\lambda_1$  is graphically determined, the obtained value always agrees with  $\lambda_1 = -A_0/A_1$ .

2074

$$\lambda_1 = - \frac{A_0}{A_1} \tag{28}$$

Now it can be seen that if  $A_0 < 0$ , then  $\lambda_1 > 0$  and the airplane is unstable.

Example:  $A_1 = 40.809$                        $A_0 = -0.3362$

From formula (28)

$$\lambda_1 = - \frac{A_0}{A_1} = - \frac{-0.3362}{40.809} = 0.00825$$

In determining  $\lambda_2$ , it must be recalled that  $\lambda_2$  is large and therefore if the powers of  $\lambda_2$  below the third are neglected, the approximate value is obtained

$$\lambda_2^4 + A_3 \lambda_2^3 \approx 0$$

whence

$$\lambda_2 \approx - A_3$$

Computations on many airplanes show that the best approximation for  $\lambda_2$  is the value<sup>11</sup>

$$\lambda_2 \approx \frac{z_p}{i_A} \tag{29}$$

Because  $i_A > 0$  and at below-stalling angles of attack  $z_p < 0$ ,  $\lambda_2 < 0$ .

By setting

$$\Delta(\lambda) = \lambda^4 + A_3 \lambda^3 + A_2 \lambda^2 + A_1 \lambda + A_0$$

<sup>11</sup>Usually the value of  $z_p/i_A$  gives a very small error in the determination of the root  $\lambda_2$ . However, a more accurate determination is necessary to compute the complex roots of the characteristic equation (more accurately, the real part).

for a more accurate determination of the root  $\lambda_2$ ,  $\Delta$  is plotted as a function of  $\lambda$  near a value equal to  $\lambda \approx l_p/i_A$ , by laying off  $\lambda$  on the abscissa and  $\Delta$  on the ordinate. The intersection of the curve  $\Delta(\lambda)$  with the abscissa gives the accurate value of  $\lambda_2$ . Because

$$\Delta'(\lambda) = 4\lambda^3 + 3A_3\lambda^2 + 2A_2\lambda + A_1$$

and as a polynomial for large numbers has the sign of its greatest term and  $\lambda_2$  is negative, usually  $\Delta'(\lambda_2) < 0$ . Hence, if after the first trial the point falls above the X-axis, the next value of  $\lambda_2$  in smaller absolute value is taken, whereas if the point falls below the X-axis the next value in greater absolute value is taken. Usually, three points are sufficient for drawing the curve  $\Delta(\lambda)$  and determining  $\lambda_2$ .

Example: Find  $\lambda_2$  from the equation

$$\lambda^4 + 8.27\lambda^3 + 12.75\lambda^2 + 40.809\lambda - 0.3362 = 0$$

Because  $l_p/i_A = -7.26$ , the value  $\lambda_2' = -7.2$  is used for the first value of  $\lambda_2'$ .

The order of computation is clear from table I.

The second, third, and fourth powers of  $\lambda$ , which are required for the computation, may be found in appendix 2, which gives the powers of numbers from 2 to 15 in steps of 0.2 and covers the entire range of values of  $\lambda$  encountered in computation. The curve  $\Delta(\lambda)$  from which  $\lambda_2 = -7.3$  is taken, is given in figure 27. After having found  $\lambda_1$  and  $\lambda_2$ , the conjugate complex roots  $\lambda_3, \lambda_4$  are obtained from the following considerations:

Equation (26) may be put in the form

$$\lambda^4 + A_3\lambda^3 + A_2\lambda^2 + A_1\lambda + A_0 = (\lambda - \lambda_1)(\lambda - \lambda_2)(\lambda^2 + a\lambda + b) = 0$$

or

$$\begin{aligned} \lambda^4 + [a - (\lambda_1 + \lambda_2)]\lambda^3 + [b - a(\lambda_1 + \lambda_2) + \lambda_1\lambda_2]\lambda^2 + \\ [a\lambda_1\lambda_2 - b(\lambda_1 + \lambda_2)]\lambda + b\lambda_1\lambda_2 = 0 \end{aligned}$$

By equating the coefficients of the same powers of  $\lambda$  the following equation is obtained:

$$A_3 = a - (\lambda_1 + \lambda_2)$$

$$A_2 = b - a(\lambda_1 + \lambda_2) + \lambda_1\lambda_2$$

$$A_1 = a\lambda_1\lambda_2 - b(\lambda_1 + \lambda_2)$$

$$A_0 = b\lambda_1\lambda_2$$

whence  $b = A_0/\lambda_1\lambda_2$ ; but by (28)  $\lambda_1 = -A_0/A_1$ , hence

$$b = -\frac{A_1}{\lambda_2} \quad (30)$$

The value of  $a$  is found from

$$A_2 = b - a(\lambda_1 + \lambda_2) + \lambda_1\lambda_2$$

$$a = \frac{b + \lambda_1\lambda_2 - A_2}{\lambda_1 + \lambda_2} \quad (31)$$

If  $a$  and  $b$  are known, the roots  $\lambda_3$  and  $\lambda_4$  are obtained from the equation

$$\lambda^2 + a\lambda + b = 0$$

$$\lambda_{3,4} = -\frac{a}{2} \pm 1 \sqrt{b - \frac{a^2}{4}}$$

If  $\lambda_3 = \xi + i\eta$ ,  $\lambda_4 = \xi - i\eta$  and<sup>12</sup>

---

<sup>12</sup>These formulas are written on the assumption that  $b > a^2/4$ ; if  $b < a^2/4$ , the formulas become

$$\lambda_{3,4} = -\frac{a}{2} \pm \sqrt{\frac{a^2}{4} - b}$$

and in this case the airplane is unstable. If  $A_1 \leq 0$ , then  $b \leq 0$  and instability results. A change in the sign of  $A_1$  is generally due to the loss of weathercock stability of the airplane.

$$\xi = -\frac{a}{2} \quad (32)$$

$$\eta = \sqrt{b - \frac{a^2}{4}} \quad (33)$$

Example: Find the complex roots of the equation

$$\lambda^4 + 8.27\lambda^3 + 12.75\lambda^2 + 40.809\lambda - 0.3362 = 0$$

It has been established that

$$\lambda_1 = +0.00825 \quad \text{and} \quad \lambda_2 = -7.3$$

From equation (30),  $b = -\frac{A_1}{\lambda_2} = -\frac{40.809}{(-7.3)} = 5.61$  and by equations (31)

$$a = \frac{b + \lambda_1\lambda_2 - A_2}{\lambda_1 + \lambda_2} = \frac{5.61 + 0.00825(-7.3) - 12.75}{0.00825 - 7.3} = 0.990$$

It can be seen with the aid of equations (32) and (33) that

$$\xi = -\left(\frac{a}{2}\right) = -\frac{0.990}{2} = -0.495$$

$$\eta = \sqrt{b - \left(\frac{a}{2}\right)^2} = 2.315$$

##### 5. MOTION CHARACTERIZED BY ROOTS $\lambda_1, \lambda_2, \lambda_3,$ AND $\lambda_4$

The disturbed motion of an airplane is characterized by the expressions

$$\beta = B_1 e^{\lambda_1 \bar{t}} + B_2 e^{\lambda_2 \bar{t}} + B_3 e^{\lambda_3 \bar{t}} + B_4 e^{\lambda_4 \bar{t}}$$

$$\bar{p} = P_1 e^{\lambda_1 \bar{t}} + P_2 e^{\lambda_2 \bar{t}} + P_3 e^{\lambda_3 \bar{t}} + P_4 e^{\lambda_4 \bar{t}}$$

$$\bar{r} = R_1 e^{\lambda_1 \bar{t}} + R_2 e^{\lambda_2 \bar{t}} + R_3 e^{\lambda_3 \bar{t}} + R_4 e^{\lambda_4 \bar{t}}$$

This motion may be broken down into three components

$$\text{I } \beta_1 = B_1 e^{\lambda_1 \bar{t}}; \bar{p}_1 = P_1 e^{\lambda_1 \bar{t}}; \bar{r}_1 = R_1 e^{\lambda_1 \bar{t}}$$

$$\text{II } \beta_2 = B_2 e^{\lambda_2 \bar{t}}; \bar{p}_2 = P_2 e^{\lambda_2 \bar{t}}; \bar{r}_2 = R_2 e^{\lambda_2 \bar{t}}$$

$$\text{III } \beta_3 = B_3 e^{\lambda_3 \bar{t}} + B_4 e^{\lambda_4 \bar{t}}, \bar{p}_3 = P_3 e^{\lambda_3 \bar{t}} + P_4 e^{\lambda_4 \bar{t}}, \bar{r}_3 = R_3 e^{\lambda_3 \bar{t}} + R_4 e^{\lambda_4 \bar{t}}$$

The computation of the coefficients  $B_1, B_2, B_3, B_4, P_1, P_2$ , and so forth will not be considered in detail. It should be noted that of all these magnitudes only four are arbitrary and are determined from the initial conditions, whereas the remainder can be obtained from these four magnitudes.

From a numerical analysis of these coefficients the following conclusions may be made:

I. Consider the group

$$\beta_1 = B_1 e^{\lambda_1 \bar{t}}$$

$$\bar{p}_1 = P_1 e^{\lambda_1 \bar{t}}$$

$$\bar{r}_1 = R_1 e^{\lambda_1 \bar{t}}$$

The magnitude  $P_1$  is small in comparison with  $B_1$  and  $R_1$ . The root  $\lambda_1$  is very small. Evidently, if the airplane is stable,  $\lambda_1 < 0$  and the magnitudes  $\beta$  (sideslip),  $p$  (angular velocity of roll), and  $r$  (angular velocity of yaw) decrease with time (with increase in  $\bar{t} = t/\tau$ ).

The root  $\lambda_1$  characterizes spiral stability of the airplane. In order to clarify the physical significance of spiral stability, the motion after a roll of the airplane is considered. Let the airplane roll in such a manner that the right wing drops. Whereas in the horizontal position of the wing the lift force balanced the force of gravity, the force of gravity will now give a projection on the Y-axis and the airplane begins to sideslip ( $\beta$ ) on the right (lowered) wing. As a result of the sideslip, two aerodynamic moments appear: the moment  $l_\beta \times \beta$  tending to rotate the wing in the horizontal position and the moment  $n_\beta \times \beta$  decreasing the sideslip angle  $\beta$ . Because of the action of the moment  $n_\beta \times \beta$  the airplane begins to yaw, that is, an angular velocity  $r$  appears, which gives rise to two new moments: the moment  $n_r \times r$  opposing the moment  $n_\beta \times \beta$  and a moment  $l_r \times r$ , which opposes the moment  $l_\beta \times \beta$ .

Thus, the characteristics  $l_\beta$  and  $n_r$  act favorably in eliminating the disturbance and the characteristics  $n_\beta$  and  $l_r$  act unfavorably (with respect to spiral stability).

As can be seen from equation (28) spiral stability is characterized by  $A_0$ , which is determined by the equation

$$A_0 = \frac{\mu}{i_A i_C} \left( l_r n_\beta - n_r l_\beta \right)$$

where

$$\mu > 0; \quad \frac{C_L}{2} > 0$$

$$l_r > 0; \quad n_\beta < 0; \quad n_r < 0; \quad l_\beta > 0$$

Hence, there will be stability for the case where  $n_r l_\beta$  in absolute value is greater than  $l_r n_\beta$  whence

$$\left| \frac{l_\beta}{n_\beta} \right| > \left| \frac{l_r}{n_r} \right|$$

The degree of stability is characterized by the time in which the initial disturbance decreases by one-half

$$e^{\lambda_1 \bar{t}} = \frac{1}{2}$$

$$\lambda_1 \bar{t} = \ln \frac{1}{2} = -0.693$$

but

$$\bar{t} = \frac{t}{\tau} \quad t_{\text{spir}} = -0.693 \frac{\tau}{\lambda_1} \quad (34)$$

In the case of instability  $\lambda_1 > 0$  and the time of decrease of the initial disturbance by one-half will be negative. In the case of stability  $\lambda_1 < 0$  and  $t_{\text{spir}}$  will be positive

$$\tau = 1.83 \text{ sec} \quad \lambda_1 = +0.00825$$

$$t_{\text{spir}} = -0.693 \frac{1.83}{0.00825} = -154 \text{ sec}$$

It has been found that 2.5 minutes after the initial instant the initial disturbance will increase to twice the value. Such motion evidently will not be observed by the pilot.

Experience shows that spiral instability is not felt by the pilot if the time of increase of the initial disturbance to twice the value is large. It is to be supposed that if

$$|t_{\text{spir}}| > 40 - 50 \text{ sec}$$

at the initial flight conditions the airplane will be satisfactory with regards to spiral stability.

II. Consider the group

$$\beta_2 = B_2 e^{\lambda_2 \bar{t}}$$

$$\bar{p}_2 = P_2 e^{\lambda_2 \bar{t}}$$

$$\bar{r}_2 = R_2 e^{\lambda_2 \bar{t}}$$

Numerical analysis shows that during a disturbance  $B_2$  and  $R_2$  are small in comparison with  $P_2$ ; that is, this group is found to characterize a motion which differs little from a pure roll. It has been shown that

$$\lambda_2 \approx \frac{l_p}{I_A}$$

and because at below-stalling angles  $l_p < 0$ ,  $\bar{p}$  will decrease very quickly with time because  $\lambda_2$  is large. Generally, at the below-stalling angles this motion is not noticeable after 1 second.

III. Consider the group

$$\beta_3 = B_3 e^{\lambda_3 \bar{t}} + B_4 e^{\lambda_4 \bar{t}}$$

$$\bar{p}_3 = P_3 e^{\lambda_3 \bar{t}} + P_4 e^{\lambda_4 \bar{t}}$$

$$\bar{r}_3 = R_3 e^{\lambda_3 \bar{t}} + R_4 e^{\lambda_4 \bar{t}}$$

Because  $\lambda_3$  and  $\lambda_4$ ,  $B_3$  and  $B_4$  are conjugate complex quantities

$$\lambda_3 = \xi + i\eta, B_3 = b_3 + ib_4 = B(\cos \beta + i \sin \beta) = B e^{i\beta}$$

$$\lambda_4 = \xi - i\eta, B_4 = b_3 - ib_4 = B(\cos \beta - i \sin \beta) = B e^{-i\beta}$$

$$B_3 e^{\lambda_3 \bar{t}} + B_4 e^{\lambda_4 \bar{t}} = B e^{i\beta} e^{(\xi + i\eta)\bar{t}} + B e^{-i\beta} e^{(\xi - i\eta)\bar{t}}$$

$$= B e^{\xi \bar{t}} [e^{(\eta \bar{t} + \beta)i} + e^{-(\eta \bar{t} + \beta)i}]$$

But  $e^{(\eta\bar{t} + \beta)i} + e^{-(\eta\bar{t} + \beta)i} = 2 \cos(\eta\bar{t} + \beta)$ ; and, therefore, if  $2B = \bar{B}$

$$\beta_3 = B_3 e^{\lambda_3 \bar{t}} + B_4 e^{\lambda_4 \bar{t}} = \bar{B} e^{\xi \bar{t}} \cos(\eta\bar{t} + \beta)$$

Similarly,

$$\bar{p} = P_3 e^{\lambda_3 \bar{t}} + P_4 e^{\lambda_4 \bar{t}} = \bar{P} e^{\xi \bar{t}} \cos(\eta\bar{t} + \gamma)$$

$$\bar{r}_3 = R_3 e^{\lambda_3 \bar{t}} + R_4 e^{\lambda_4 \bar{t}} = \bar{R} e^{\xi \bar{t}} \cos(\eta\bar{t} + \delta)$$

This group characterizes the oscillatory damping of the motion.

The time required for decreasing the amplitude by one-half can now be found.

$$e^{\xi \bar{t}_2} = \frac{1}{2}$$

$$\xi \bar{t}_2 = -0.693 \qquad \bar{t}_2 = \frac{t_2}{\tau}$$

Therefore

$$t_2 = -0.693 \frac{T}{\xi} \qquad (35)$$

Example:  $\tau = 1.83 \qquad \xi = -0.495$

$$t_2 = -0.693 \frac{1.83}{(-0.495)} = 2.56 \text{ sec}$$

The period of oscillation is determined from the relations

$$\eta \bar{T} = 2\pi$$

$$\bar{T} = \frac{T}{\tau} \qquad (36)$$

$$T = 2\pi \frac{T}{\eta}$$

Example:  $\tau = 1.83$  sec       $\eta = 2.31$

$$T = 6.28 \frac{1.83}{2.31} = 4.98 \text{ sec}$$

With regard to the oscillatory stability of the airplane, the following condition must be imposed: The airplane should be stable in oscillation and the time of decrease of the initial disturbance by one-half ( $t_2$ ) should be less than  $1 \div 1.5$  times the oscillation period

$$t_2 < 1 \div 1.5T$$

The stability in oscillation is affected mainly by the lateral static stability  $n_\beta$ . The other coefficients also affect the oscillation of the airplane but to a smaller extent. Whereas an airplane may have a small static instability, it may nevertheless be dynamically stable but the period of oscillation ( $T$ ) and the time of decrease of the initial disturbance by one-half ( $t_2$ ) will be large. At greater static instability, the airplane will be unstable in oscillation; that is, the amplitude of oscillation of such an airplane will increase with time. For a coefficient of lateral static stability of the order  $n_\beta = 0.01$  and greater, the least disturbance will tend to increase the roll of the airplane (a kind of slow spin). Whereas from tests in the wind tunnel of the model with locked controls it was found that the airplane is neutral or even has a small weathercock stability, in flight such an airplane will be unstable because of the mobility of the control surface. For this reason, from the requirement of oscillatory stability it follows that the airplane should be statically stable over the entire range of flight angles of attack and especially at below-stalling angles of attack.

## 6. ORDER OF COMPUTATION OF DYNAMIC STABILITY

### Computation of Airplane Northrop 2E for Dynamic Stability

In this section, the entire dynamic-stability computation is presented from setting up tables of the structural parameters to obtaining the final dynamic stability characteristics. At the start of the computation, a table must be set up in which all parameters of the airplane required for computing the lateral dynamic stability are included.

I.  $G$ , weight of airplane, kilograms

II. Wing

1.  $b$ , wing span, meters
2.  $b_{mw}$ , midwing-section span, meters
3.  $S$ , wing area, square meters
4.  $c_0$ , chord at root, meters
5.  $c_t$ , chord at tip, meters
6.  $\Psi$ , dihedral angle - angle between plane of chords and plane perpendicular to plane of symmetry of airplane and passing through the chord at the tip, degrees (fig. 15)
7.  $X$ , sweptback angle - angle between lines passing through focal line taken at one-quarter chord from leading edge of wing and plane perpendicular to axis of fuselage ( $X > 0$  for forward sweepback), degrees (fig. 19)
8.  $\gamma$ , angle of twist of wing, degrees

III. Vertical tail surface

1.  $S_{tf}$ , vertical tail surface area (area of tail with part of fuselage, (fig. 11), square meters
2.  $b_t$ , tail span (measurement shown in fig. 11), meters
3.  $l_t$ , distance from center of gravity to hinge of rudder, meters
4. Angle between line of zero lift and line joining center of gravity of airplane with geometric center of vertical tail surface (with part of fuselage)

IV. Fuselage

1.  $S_f$ , area of projection of fuselage on plane of symmetry of airplane, square meters

2.  $l_f$ , length of fuselage, meters
3.  $h$ , maximum height of projection of fuselage on plane of symmetry, meters
4.  $l_{nf}$ , distance of center of gravity from nose of fuselage, meters

The magnitudes computed under I, II, III, and IV are always positive.

The table of structural parameters for the Northrop airplane is:

$G = 2600$ kilograms	$S_{tf} = 3.11$ square meters
$S = 33.4$ square meters	$b_t = 1.88$ meters
$b = 14.53$ meters	$l_t = 5.65$ meters
$b_{mv} = 3.29$ meters	$S_f = 11.69$ square meters
$c_0 = 2.9$ meters	$l_f = 8.67$ meters
$c_K = 1.5$ meters	$h = 1.45$ meters
$\psi = 7^\circ 30'$	$l_{nf} = 2.11$ meters
$\chi = 2^\circ 30'$	$\alpha = 12^\circ$
$\gamma = 1^\circ 30'$	

The airplane is a low-wing single-engine type

$$\frac{G}{S} = 78 \text{ kg/m}^2 \quad \frac{S_{tf}}{S} = 0.093 \quad \frac{l_f}{h} = 6$$

$$\eta = \frac{c_0}{c_t} = 1.94 \quad \frac{l_t}{b} = 0.389 \quad \frac{S_f}{S} = 0.35$$

$$\lambda = \frac{b^2}{S} = 6.34 \quad \lambda_t = 1.14 \quad \frac{b_{mv}}{b} = 0.226$$

$$\mu = 2.2 \frac{G}{S} = 11.8 \quad \frac{l_{nf}}{l_f} = 0.244$$

### Determination of Aerodynamic Coefficients

1. The curve of variation of the coefficient of lift ( $C_L$ ) against the angle of attack ( $\alpha$ ) obtained from tests in the wind tunnel for a model of the Northrop airplane is given in figure 2. The angle of attack is measured from the wing chord. Because  $C_L$  must be determined for angles of attack measured from the line of zero-lift, table II is obtained.

2. The rotary derivatives  $l_p$ ,  $l_r$ ,  $n_p$ , and  $n_r$  were determined from the aforementioned equations and curves and also experimentally on a special apparatus (reference 11).

#### (a) Determination of $l_p$

The derivative  $l_p$  is obtained from the data of the table of structural parameters (fig. 6). The curves experimentally obtained and by figure 6 are given in figure 30. Theoretically, the derivative  $l_p$  does not depend on the angle of attack but during a test a certain change in  $l_p$  with change in  $\alpha_a$  is usually obtained. The agreement obtained, as shown in figure 30, is sufficiently good and for computing the dynamic stability the value of  $l_p$  may be taken from figure 6 without resorting to experiment.

#### (b) Determination of $n_p$

The theoretical value of  $n_p$  is found from figure 8 by using the given  $\eta$  and  $\lambda$  in the table of structural parameters. The value of  $n_p/\alpha_a$  taken from figure 8 must be multiplied by  $\alpha_a$  (angle of attack in deg. from the zero lift line). The values of  $n_p$  obtained from test and from figure 8 are given in figure 31. It is obvious that a rather large disagreement results. A systematic numerical analysis of the dynamic stability equations shows, however, that the dynamic stability characteristics depend little on the value of  $n_p$  and for this reason only an approximate value of  $n_p$  need be known. Hence, for computing the dynamic stability, the value, which is obtained from figure 8, may be used with sufficient accuracy.

#### (c) Determination of $l_r$

The determination of the derivative  $l_r$  must be divided into the following three stages:

- (1) Determination of  $l_r$  for an untwisted wing
- (2) Determination of the correction on  $l_r$  due to the twist of the wing
- (3) Determination of the part of  $l_r$  due to the vertical tail surface

1. The derivative  $l_r$  is obtained from figure 10 by the given  $\eta$  and  $\lambda$  of the wing. The value  $l_r/\alpha_a$  taken from figure 10 must be multiplied by  $\alpha_a$  (from the line of zero lift). The curve of  $l_r$  against  $\alpha_a$  for the Northrop wing is presented in figure 32. The dashed curve gives  $l_r$  for the wing without twist.

2. As the Northrop wing is aerodynamically twisted such that the angle of attack at the tip of the wing is greater than the angle of attack at the tip of the midwing by  $1.5^\circ$ , figure 12 must be used to determine the correction. This correction evidently does not depend on the angle of attack and therefore the entire straight line undergoes parallel displacement. The correction for twist is

$$l_{p, \text{ twist}} = 0.0144$$

3. The correction on  $l_r$  due to the vertical tail surface is obtained from equation (14). The required value of  $a_t$  is determined from figure 11. The continuous line in figure 32 shows the derivative  $l_r$  of the Northrop airplane with account taken of the twist of the wing and of the vertical tail surface. The figure also gives the points obtained from experiment. It is apparent that the agreement is good and that the derivative  $l_r$  may be computed theoretically without recourse to experiment.

- (d) Determination of  $n_r$

The derivative  $n_r$  is made up of a part due to the fuselage with vertical tail surface and a part due to the wing. The part  $n_r$  due to the fuselage with tail is computed from equation (16a).

The value  $a_t$  is obtained from figure 11. The part  $n_r$  due to the wing is computed from the data presented in figure 15. In order to obtain  $n_r$ , the value  $n_r/\alpha_a^2$  from figure 15 must be multiplied by the square of the angle of attack. The angle of attack must be in degrees and measured from the zero-lift line. The sum of these two parts gives the derivative  $n_r$  of the airplane. The values of the derivative  $n_r$  for the Northrop airplane obtained from test and from computation are shown in figure 33.

It should be remembered that the derivative  $n_r$  plays a great part in computing lateral dynamic stability and for this reason it is desirable that  $n_r$  be computed as accurately as possible. Remembering also that equation (16a) may in certain cases give a large error, this magnitude must be experimentally determined.

(e) Static derivatives  $y_\beta$ ,  $l_\beta$ ,  $n_\beta$

The static derivatives are determined from standard wind-tunnel tests; therefore these magnitudes as a rule must be obtained as shown in section 3. The values of  $y_\beta$  obtained by equation (22) (curve) and by experiment (points) are presented in figure 34. Equation (22) generally gives a sufficiently accurate value of  $y_\beta$ . The values of  $l_\beta$  for the Northrop airplane obtained from test and from computation are given in figure 35. The upper dashed curve gives  $l_\beta$  for the value  $\psi = 7.25^\circ$  (dihedral angle). In order to take account geometrically of the effect of the fuselage for a low wing in the formula, the dihedral must be decreased, as has been pointed out, by  $2^\circ$  to  $5^\circ$ . An airplane is considered the chassis of which is not streamlined and all projecting parts on the lower surface increase the effective dihedral; therefore, for the computation, the  $\psi$  angle minus  $3^\circ$  is used, that is, an angle of  $4.25^\circ$ . The lower dashed curve in figure 35 gives the value of  $l_\beta$  obtained from computation ( $\psi_{ef} = 4.25^\circ$ ). The value  $\partial l_\beta / \partial \psi$  is obtained for the given  $\eta$  and  $\lambda$  from figure 18.

The effect of the midwing on the derivative is taken into account by the decrease in  $\partial l_\beta / \partial \psi$  by an amount that may be obtained by use of equation (18). The center line in figure 35 gives the value of  $l_\beta$  with account taken of the part due to the vertical tail surface and the continuous line gives the value  $l_\beta$ , if the sweep-back of the wing is considered.

The values of  $n_\beta = \partial C_n / \partial \beta$  obtained from test and by equation (21) are given in figure 36. In equation (21), the value  $K_t = 0.8$  is used; the value of the coefficient  $K_\beta$  is obtained from figure 22 and  $a_t$  from figure 11.

Notwithstanding the sufficiently good agreement that was obtained for the Northrop airplane by computation and test for the values  $l_\beta = \partial C_l / \partial \beta$  and  $n_\beta = \partial C_n / \partial \beta$ , these formulas must be considered only approximate and in all cases the values  $l_\beta$  and  $n_\beta$  determined from the test curves  $C_n = f(\beta)$  and  $C_l = f_l(\beta)$ .

#### Moments of Inertia of the Northrop Airplane

The moments of inertia, as has been previously stated, may be obtained by computation. For the Northrop airplane, the moments of inertia are determined by full-scale experiments according to the method explained in the report by U. A. Pobyedonostsev (reference 13). The results of the investigation are as follows:

$$i_A = 0.0579, \quad i_C = 0.0959$$

where the values are given in nondimensional form.

For convenience of computation, a table of all coefficients that enter the characteristic equation must be set up as shown in table 3, in which for the derivatives the test values were taken and the angle  $\alpha_a$  was computed from the line of zero-lift.

From the data of table 3, the coefficients of the characteristic equation  $A_3, A_2, A_1,$  and  $A_0$  are computed by equations (27). The values of these coefficients for the Northrop airplane computed for the angles of attack  $\alpha_a = 1^\circ, 5^\circ, 9^\circ,$  and  $13^\circ$  are given in table 4 and the values  $\lambda_1, \lambda_2, \xi,$  and  $\eta$ , computed by the equations of section 4, are given in figures 37 and 38. A comparison of the computed results with flight tests of reference 14 is made in figure 39.

Complete agreement was obtained for the period of oscillation  $T$ . The disagreement that exists for  $t_2$  (the time of decrease of the amplitude to 1/2) may be explained by the fact that no account was taken in the computation of the effect of the propeller slipstream

on the vertical tail surface. The magnitudes  $\lambda_1$  and  $\lambda_2$  in flight have not been determined; thus it is impossible to check the accuracy of the computations of these values. It can be seen from figure 39 that the computation gives sufficiently good results.

## 7. APPROXIMATE FORMULAS

In this section, equations are given for estimating roots quickly from the given aerodynamic coefficients. These formulas may also be used in computing the corrections on  $\lambda_1$ ,  $\lambda_2$ ,  $\xi$ , and  $\eta$  if after computing the lateral dynamic stability it is decided to change the area of the vertical tail surface or the dihedral of the wing.

For the root  $\lambda_2$ , the equation  $\lambda_2 = l_p/i_A$  can be used. The approximate expression for  $\lambda_1$ , which determines the spiral stability, is obtained from  $\lambda_1 = -A_0/A_1$  and because

$$A_1 \approx \mu \left[ \frac{l_\beta}{i_A} \left( \frac{C_L}{2} - \frac{n_p}{i_C} \right) + \frac{n_\beta}{i_C} \frac{l_p}{i_A} \right]$$

therefore

$$\lambda_1 = - \frac{\frac{C_L}{2} (l_\beta n_r - l_r n_\beta)}{l_\beta \left( \frac{C_L}{2} i_C - n_p \right) + n_\beta l_p} \quad (37)$$

The time of decrease of the initial disturbance to 1/2 is obtained by the equation

$$t_{\text{spir}} = - 0.693 \frac{1}{\lambda_1}$$

For the magnitude  $\xi$  (giving the time of decrease in the amplitude of oscillation  $t_2$  to 1/2) the following equation can be used:

$$\xi = \frac{\frac{n_r}{i_C} - \frac{y_\beta}{2} - \lambda_1}{2} \quad (38)$$

It can be seen from equation (38) that the value of  $\xi$  increases in absolute value with increase in magnitude of the damping of the yaw  $n_r$  and the value  $y_\beta$ , which characterizes the lateral force in sideslip. The magnitude of  $\xi$  drops in absolute value with increase in  $i_C$  of the nondimensional radius of inertia about the Z-axis. Vibrational instability will occur for  $\xi > 0$  and, as can be seen from equation (38), vibrational instability may be obtained for a large spiral stability if  $\lambda_1 \ll 0$ , which is usually obtained for large values of the derivative  $l_\beta$  and in the absence of weathercock stability, that is, when  $n_\beta \geq 0$ . For this reason, when the airplane has small weathercock stability or instability, the wings should not be given a large transverse dihedral because the derivative  $l_\beta$  will then be large and this condition will lead to excessive spiral stability and, what is particularly important, may give rise to oscillatory instability.

If the area of the vertical tail surface is changed, the change in  $n_r$  is obtained by the equation

$$\Delta n_r = -1.6a_t \left(\frac{l_t}{b}\right)^2 \frac{\Delta S_{tF}}{S}$$

where

$$a_t = (\partial C_L / \partial \alpha)_t \quad (\text{obtained from fig. 11})$$

$l_t$  distance from hinge of rudder to center of gravity

$\Delta S_t$  change in vertical tail surface area ( $\Delta S > 0$  for increase in area;  $\Delta S < 0$  for a decrease)

The change in  $\xi$  is obtained from the equation  $\Delta \xi \approx \Delta n_r / 2i_C$ . The new value of  $\xi$  is obtained from  $\xi' = \xi + \Delta \xi$ . From the newly obtained value  $\xi'$ ,  $t_2$  is found from equation (35).

$$t_2 = -0.693 \frac{\tau}{\xi'}$$

where  $\tau = 1.1 (G/S)/V$  (for an altitude of 3000 m).

2074

Because  $A_1$  may be approximately determined by the equation

$$A_1 \approx \mu \left[ \frac{l_\beta}{i_A} \left( \frac{C_L}{2} - \frac{n_p}{i_C} \right) + \frac{n_\beta}{i_C} \frac{l_p}{i_A} \right]$$

and

$$\lambda_1 \approx \frac{l_p}{i_A} n \approx \sqrt{b}, \text{ where } b = -\frac{A_1}{\lambda_2}$$

the following equation is obtained:

$$\eta \approx \sqrt{\mu \left[ -\frac{l_\beta}{l_p} \left( \frac{C_L}{2} - \frac{n_p}{i_C} \right) - \frac{n_\beta}{i_C} \right]} \quad (39)$$

whence the period  $T$  is determined by the equation

$$T = 6.28 \frac{T}{\eta}, \text{ where } \tau = 1.1 \frac{G}{V}$$

The greater  $\eta$  is the smaller the period of oscillation is found to be and therefore the period decreases with decrease in the absolute value of the derivative  $n_\beta$ , with increase in  $i_C$ , the non-dimensional radius of inertia with respect to the Z-axis, and with decrease in the value of the derivative  $l_\beta$ . If the expression under the square root sign becomes negative (as may occur in the case where  $n_\beta > 0$ , that is, in the absence of weathercock stability) the magnitude  $\eta$  does not characterize the period of oscillation but together with the magnitude  $\xi$  determines the asymptotic deviation of the airplane from its course.

The previously derived approximate equations give very good agreement with exact computation for the Northrop 2-E airplane. In other cases, generally speaking, the agreement may be less complete but a qualitatively correct result will be obtained<sup>13</sup>.

---

<sup>13</sup>At the time the present article was being prepared for publication the previously derived formulas were checked for a large number of airplanes. In almost all cases the approximate formulas give very good agreement with the exact formulas and they may therefore be used in computing the lateral dynamic stability of the airplanes.

## APPENDIX 1

Up to the present time investigations in the wind tunnel have been conducted in a system of axes different from that assumed in this paper and for this reason equations are presented herein with the aid of which the old coefficients may be reduced to the coefficients used in this paper.

The sideslip angle  $\beta$  (previously  $\gamma$ ) in the diagrams of the wind-tunnel tests has the same sign as  $\beta$  assumed in the report. The moment coefficients have the opposite sign. Moreover, up to this time the moment coefficients were referred to  $\rho V^2$  in order to reduce them to nondimensional coefficients. If the yawing moment (in the old notation  $C_{my}$ ) is based on the distance between the center of gravity and the rudder hinge and the rolling moment ( $C_{mx}$ ) is based on the span,

$$C_l = -2C_{mx} \quad C_n = -2 \frac{l_t}{b} C_{my} \quad C_y = -2C_z$$

If the results from the tunnel investigations ( $C_{mx}$ ,  $C_{my}$ ,  $C_z$ ) are given in a gravity system of coordinates  $\partial C_{mx}/\partial \beta$ ,  $\partial C_{my}/\partial \beta$ , and  $\partial C_z/\partial \beta$  are obtained from the curves and the coefficients  $l_\beta$ ,  $n_\beta$ , and  $y_\beta$  are obtained from the equations

$$l_\beta = \frac{\partial C_l}{\partial \beta} = -2 \frac{\partial C_{mx}}{\partial \beta} \times 57.3$$

$$n_\beta = \frac{\partial C_n}{\partial \beta} = -2 \frac{l_t}{b} \frac{\partial C_{my}}{\partial \beta} \times 57.3; \quad y_\beta = \frac{\partial C_y}{\partial \beta} = -2 \frac{\partial C_z}{\partial \beta} \times 57.3$$

If the results are given in a system of chord axes, all moments and forces are based on  $\rho V^2$ , the rolling moment  $C'_{mx}$  is based on the span, and the moment of yaw  $C'_{my}$  is based on  $l_t$  (the distance between the center of gravity and the hinge of the rudder),

$$C_{mx} = C'_{mx} \cos \alpha + \frac{l_t}{b} C'_{my} \sin \alpha; \quad C_{my} = C'_{my} \cos \alpha - \frac{l_t}{b} C'_{mx} \sin \alpha$$

$$C_z = C'_z$$

2074

and finally

$$l_{\beta} = \frac{\partial C_l}{\partial \beta} = -2 \frac{\partial C_{mx}}{\partial \beta} 57.3 = -2 \left[ \frac{\partial C'_{mx}}{\partial \beta} \cos \alpha + \frac{l_t}{b} \frac{\partial C'_{my}}{\partial \beta} \sin \alpha \right] 57.3$$

$$n_{\beta} = \frac{\partial C_n}{\partial \beta} = -2 \left[ \frac{l_t}{b} \frac{\partial C'_{my}}{\partial \beta} \cos \alpha - \frac{\partial C'_{mx}}{\partial \beta} \sin \alpha \right] 57.3$$

$$y_{\beta} = \frac{\partial C_y}{\partial \beta} = -2 \frac{\partial C'_z}{\partial \beta} \times 57.3$$

APPENDIX 2

SECOND, THIRD AND FOURTH POWERS OF NUMBERS FROM 2.0 TO 15.0

60

$\lambda$	$\lambda^2$	$\lambda^3$	$\lambda^4$	$\lambda$	$\lambda^2$	$\lambda^3$	$\lambda^4$	$\lambda$	$\lambda^2$	$\lambda^3$	$\lambda^4$
2.0	4.00	8.000	16.000	6.6	43.56	287.5	1897.5	11.0	121.0	1331.0	14641.0
2.2	4.84	10.65	23.43	6.8	46.24	314.4	2138.1	11.2	125.4	1405.0	15735.2
2.4	5.76	13.82	33.18					11.4	130.0	1481.5	16890.0
2.5	6.76	17.58	45.70	7.0	49.00	343.0	2401	11.6	134.5	1561.0	18106.4
2.8	7.84	21.95	61.47	7.2	51.84	373.2	2687.4	11.8	139.2	1643.0	19387.8
				7.4	54.76	405.2	2998.7				
3.0	9.00	27.00	81.00	7.6	57.76	439.0	3336.2	12.0	144.0	1728.0	20736.0
3.2	10.24	32.77	104.86	7.8	60.84	474.5	3701.5	12.2	148.8	1816.0	22153.3
3.4	11.56	39.30	133.63					12.4	153.8	1906.6	23642.1
3.6	12.96	46.66	168.0	8.0	64.00	512.0	4096	12.6	158.8	2000.4	25117.4
3.8	14.44	54.87	208.5	8.2	67.24	551.4	4521.2	12.8	163.8	2097.0	26843.5
				8.4	70.56	592.7	4978.7				
4.0	16.00	64.00	256.0	8.6	73.96	636.0	5470.1	13.0	169.0	2197.0	28561.0
4.2	17.64	74.09	311.2	8.8	77.44	681.5	5996.9	13.2	174.2	2300.0	30350.6
4.4	19.36	85.18	374.8					13.4	179.6	2406.1	32256.0
4.6	21.16	97.34	447.7	9.0	81.00	729.0	6561	13.6	185.0	2515.5	34210.2
4.8	23.04	110.6	530.8	9.2	84.64	778.7	7163.9	13.8	190.4	2628.0	36267.4
				9.4	88.36	830.6	7807.5				
5.0	25.000	125.0	625.0	9.6	92.16	884.7	8493.5	14.0	196.0	2744.0	38416.0
5.2	27.04	140.6	731.2	9.8	96.04	941.2	9223.7	14.2	201.6	2863.3	40658.7
5.4	29.16	157.5	850.3					14.4	207.4	2986.0	42998.2
5.6	31.36	175.6	983.4	10.0	100.0	1000.0	10000	14.6	213.2	3112.1	45437.2
5.8	33.64	195.1	1131.6	10.2	104.0	1061.2	10824.3	14.8	219.0	3242.0	47978.6
				10.4	108.1	1125.0	11698.6				
6.0	36.00	216.0	1296	10.6	112.4	1191.0	12624.8	15.0	225.0	3375.0	50625.0
6.2	38.44	238.3	1477.6	10.8	116.6	1259.7	13604.9				
6.4	40.96	262.1	1677.9								

NACA TM 1264

## REFERENCES

1. Vedrov, V. S.: Dynamic Stability of the Airplane. Oborongiz, 1938.
2. Loitsyansky, L. G., and Lurie, A. I.: Course in Theoretical Mechanics. Vol. 1. GITI, 1932, p. 250.
3. Gos, F.: Stability and Maneuverability of Airplanes. ONII, 1934, p. 187.
4. Polyadsky: Rep. No. 412, CAHI, 1939.
5. Pearson, Henry A., and Jones, Robert T.: Theoretical Stability and Control Characteristics of Wings with Various Amounts of Taper and Twist. NACA Rep. 635, 1938.
6. Targ, S. M.: Investigation of the Vertical Tail Surface Operation. Tech. Note No. 31, CAHI, 1935.
7. Shortal, Joseph A.: Effect of Tip Shape and Dihedral on Lateral-Stability Characteristics. NACA Rep. 548, 1935.
8. Weick, Fred E., and Jones, Robert T.: The Effect of Lateral Controls in Producing Motion of an Airplane as Computed from Wind-Tunnel Data. NACA Rep. 570, 1936.
9. Zimmerman, Charles H.: An Analysis of Lateral Stability in Power-Off Flight With Charts for Use in Design. NACA Rep. 589, 1937.
10. Diehl, Walter Stuart: Engineering Aerodynamics. The Ronald Press Co., 2d ed., 1936.
11. Raikh, A. L.: Theory and Method of Experimental Determination of the Rotational Derivatives. Rep. No. 419, CAHI, 1939.
12. Nikityuk, A. I.: Methods of the Analytical Computation of the Moments of Inertia of an Airplane. Tech. Vozdushnogo, Flota No. 5, 1931.
13. Pobyedonostsev, U. A.: Experimental Determination of the Moments of Inertia of an Airplane. Rep. No. 201, CAHI, 1935.
14. Kalachev, G. S.: Flight Tests of a Northrop 2E Airplane. Tech. Note No. 167, CAHI, 1938.

TABLE I

		$\lambda' = -7.2$		$\lambda'' = -7.4$		$\lambda''' = -7.3$	
n	$A_n$	$\lambda^n$	$A_n \lambda^n$	$\lambda''^n$	$A_n \lambda''^n$	$\lambda'''^n$	$A_n \lambda'''^n$
4	1	2687.38	2687.38	2998.66	2998.66	2839.8	2839.8
3	8.27	-373.248	-3086.76	-405.224	-3351.2	-389.02	-3217.2
2	12.75	51.84	660.96	54.76	698.19	53.29	679.4
1	40.809	-7.2	-293.82	-7.4	-301.98	-7.3	-297.9
0	-0.3362	1	-0.34	1	-0.34	1	-0.34
			-32.58		43.33		3.76

TABLE II

$\alpha_a^\circ$	1°	5°	9°	13°
$C_L$	0.092	0.44	0.74	1.04

TABLE III - COEFFICIENTS FOR COMPUTING  
DYNAMIC STABILITY OF NORTHROP AIRPLANE

	$\alpha_a = 1^\circ$	$\alpha_a = 5^\circ$	$\alpha_a = 9^\circ$	$\alpha_a = 13^\circ$
$y_\beta$	0.53	0.53	0.48	0.45
$l_\beta$	0.068	0.068	0.068	0.068
$n_\beta$	-0.038	-0.037	-0.03	-0.032
$l_p$	-0.45	-0.45	-0.42	-0.38
$l_r$	0.042	0.115	0.180	0.26
$n_p$	-0.019	-0.034	-0.05	-0.065
$n_r$	-0.055	-0.0675	-0.073	-0.069
	$\frac{1}{i_A} = 17.3; \frac{1}{i_C} = 10.4$			

TABLE IIIa

	$\alpha_a = 1^\circ$	$\alpha_a = 5^\circ$	$\alpha_a = 9^\circ$	$\alpha_a = 13^\circ$
$\frac{C_L}{2}$	0.046	0.22	0.37	0.52
$\frac{y_\beta}{2}$	0.265	0.265	0.24	0.225
$\frac{l_\beta}{i_A}$	1.175	1.175	1.175	1.175
$\frac{n_\beta}{i_C}$	-0.396	-0.385	-0.312	-0.333
$\frac{l_p}{i_A}$	-7.8	-7.8	-7.27	-6.57
$\frac{l_r}{i_A}$	0.727	1.99	3.11	4.5
$\frac{n_p}{i_C}$	-0.197	-0.354	-0.052	-0.676
$\frac{n_r}{i_C}$	-0.572	-0.702	-0.76	-0.717
	$\mu = 11.8$			

2074

TABLE IV

$\alpha_a$ \ $A_n$	$A_3$	$A_2$	$A_1$	$A_0$
1	8.637	11.5	41.04	0.209
5	8.747	12.89	44.43	0.1524
9	8.27	12.75	40.809	-0.3362
13	7.51	13.32	44.14	-4.025

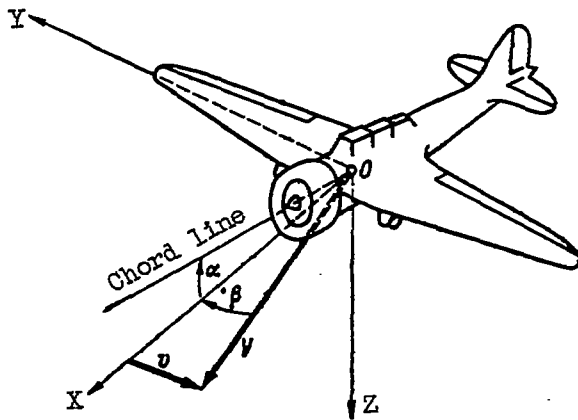


Figure 1. - System of coordinate axes.

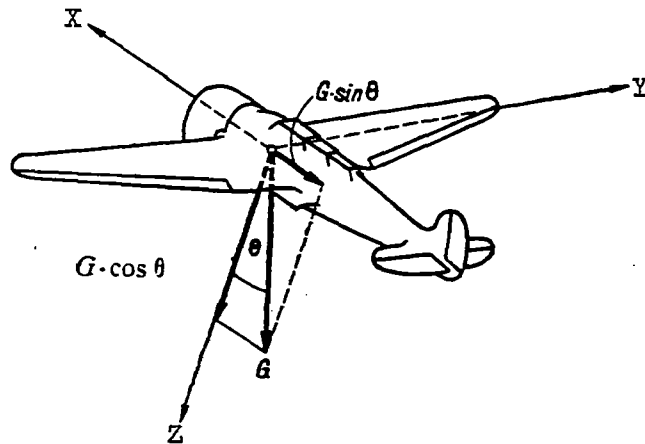


Figure 2. - Projection of gravity force on axis in symmetric flight.

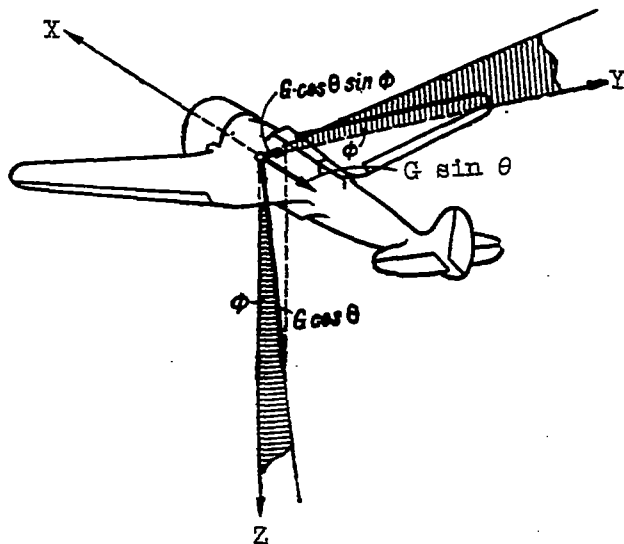


Figure 3. - Projection of gravity force on axis during roll of airplane.

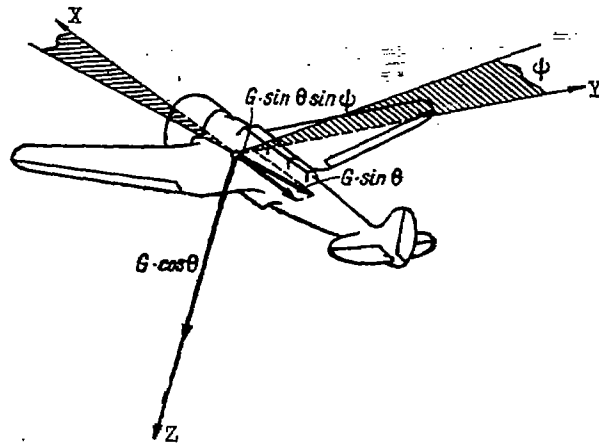


Figure 4. - Projection of gravity force on axis during yaw by angle  $\psi$ .

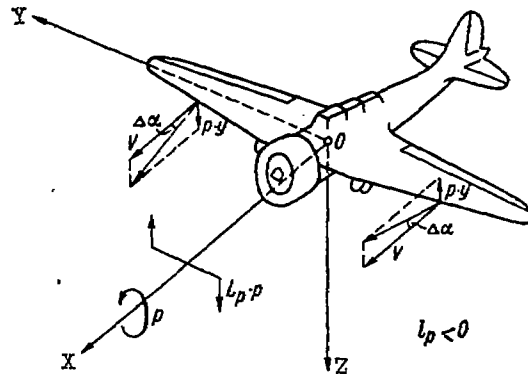


Figure 5. - Rotary derivative  $l_p$ .

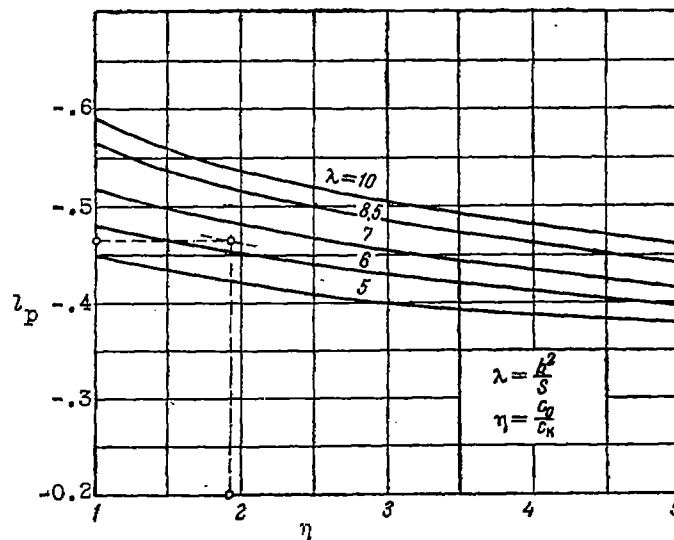


Figure 6. - Value of derivative  $l_p$  for wings of various aspect ratios and tapers.

2074

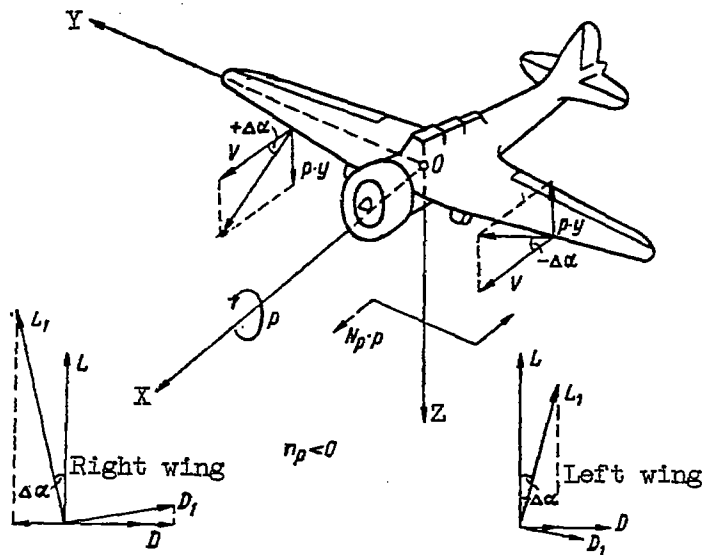


Figure 7. - Derivative  $n_p$ .

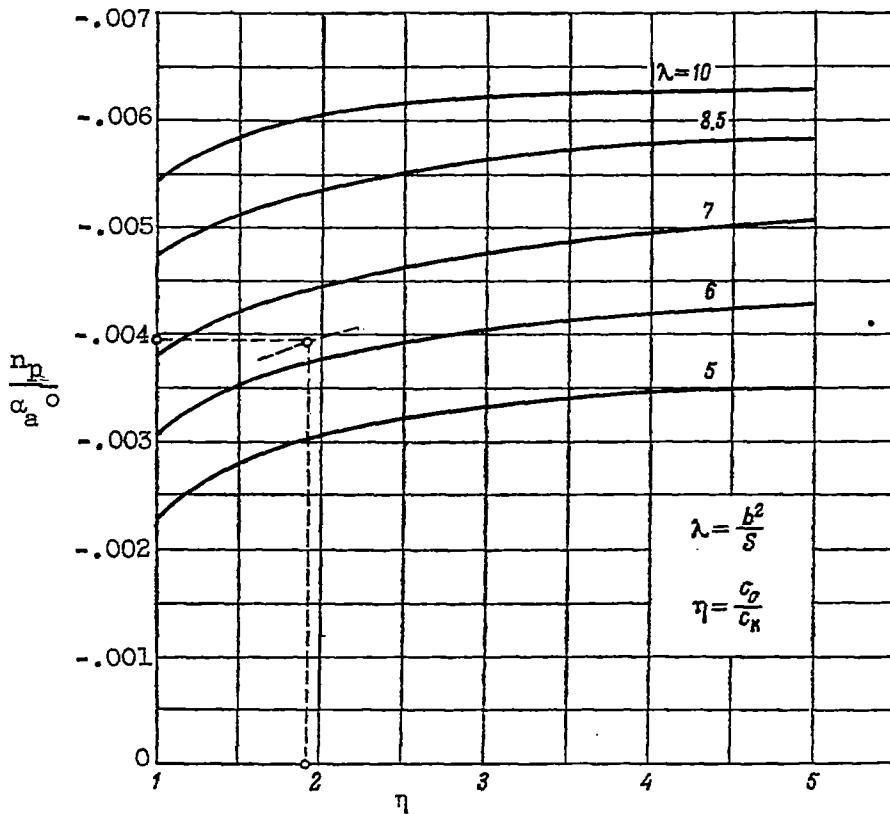
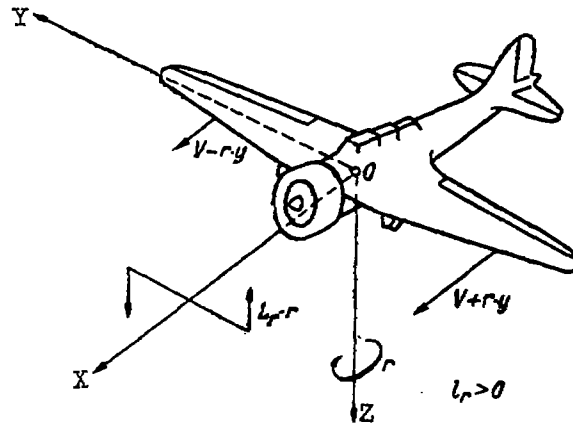
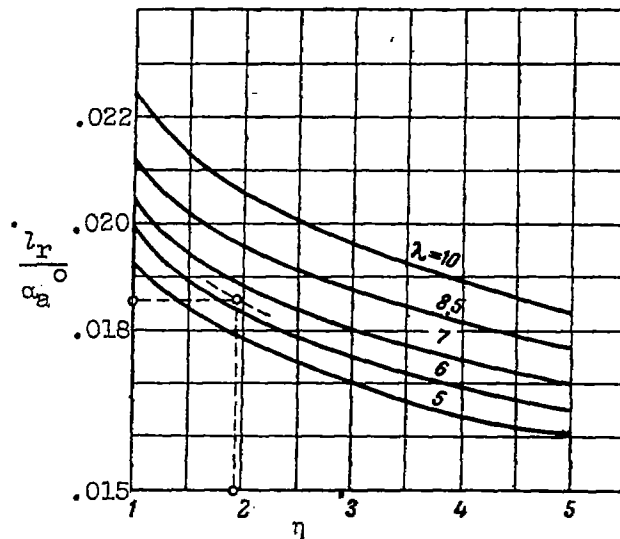


Figure 8. - Values of  $n_p/\alpha_0$  for wings of various aspect ratios and tapers.

Figure 9. - Derivative  $l_{rr}$ .Figure 10. - Values of  $l_r / \alpha_a$  for wings of various aspect ratios and tapers.

2074

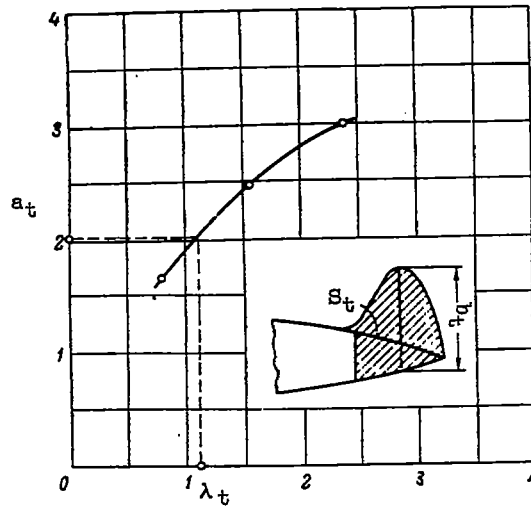


Figure 11. - Value of  $a_t = (\partial C_{L_t} / \partial \alpha)_t$  for various aspect ratios of vertical tail surface.

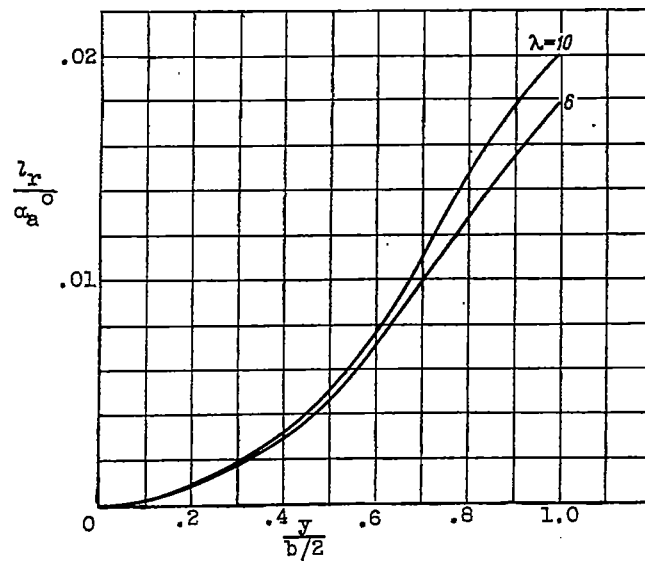


Figure 12. - Graphs for determining correction on  $l_r$  due to twist of wing.

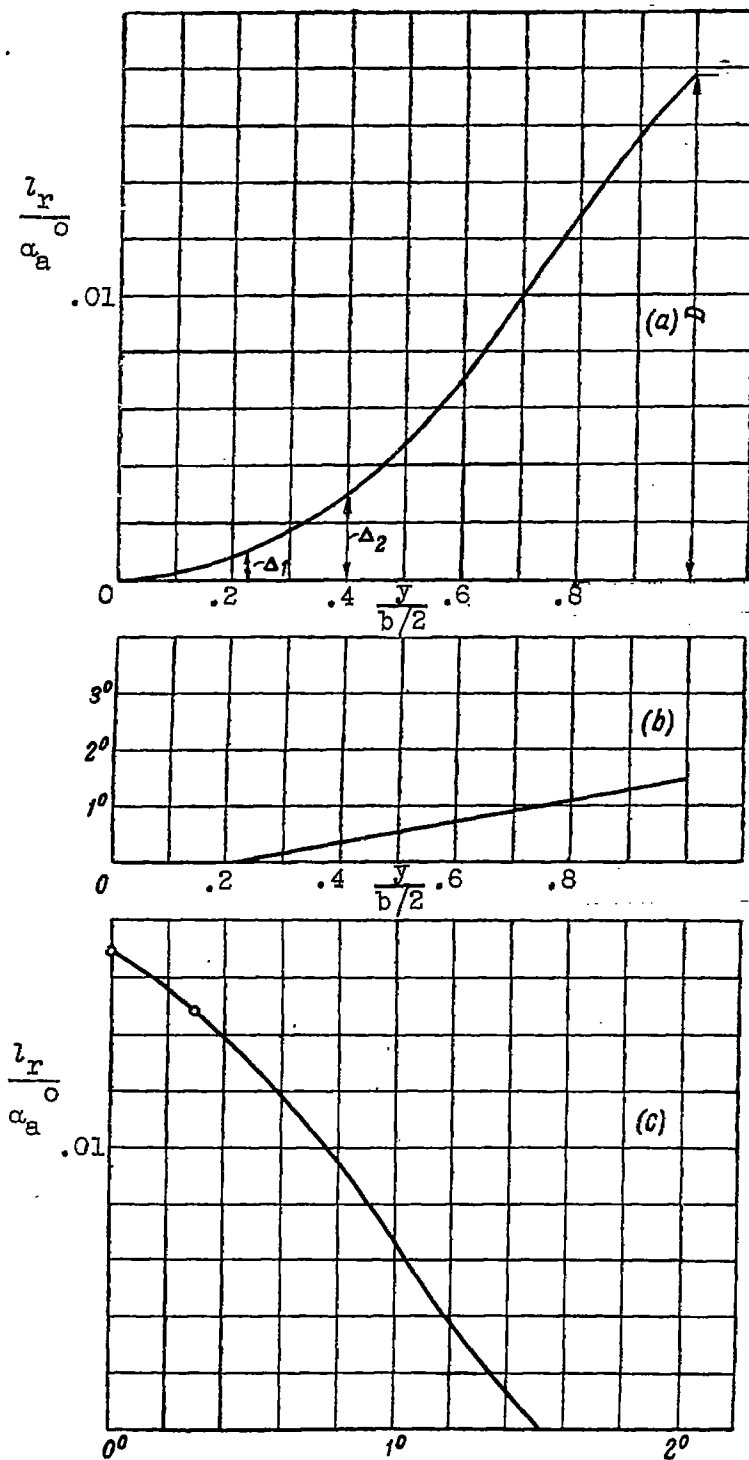


Figure 13. - Determination of correction on  $l_r$  for twist of wing.

2074

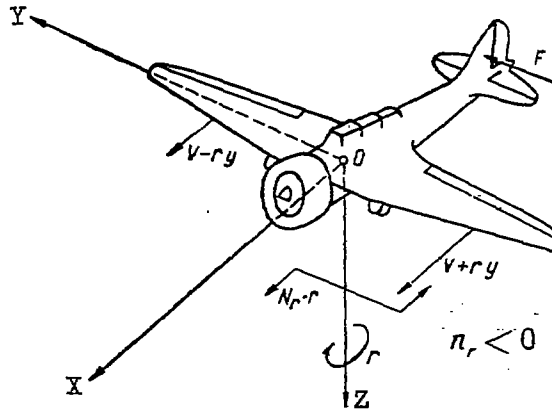


Figure 14. - Derivative  $n_r$ .

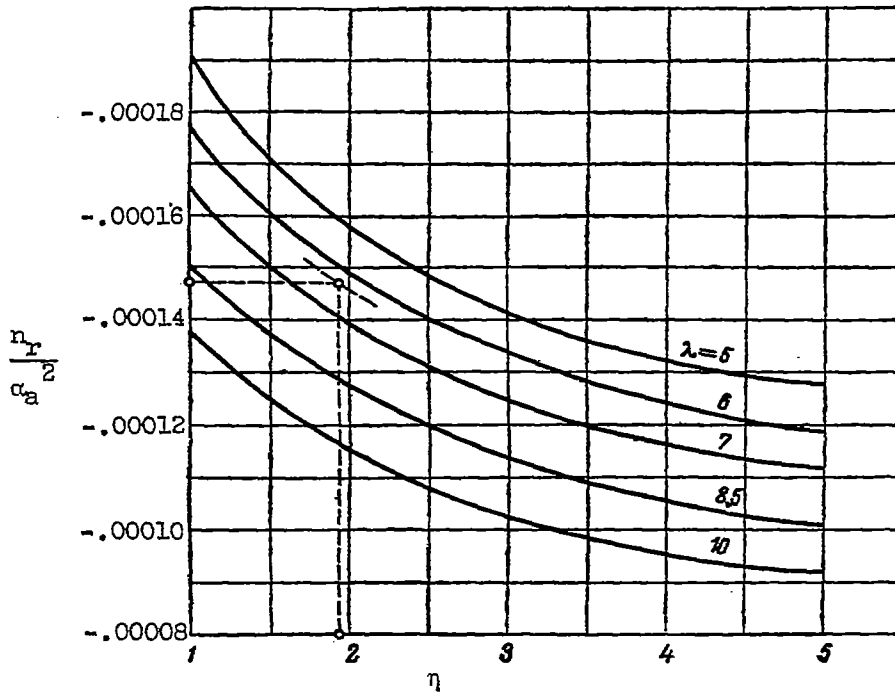


Figure 15. - Values of  $n_r/\alpha_a^2$  for wings of various aspect ratios and tapers.

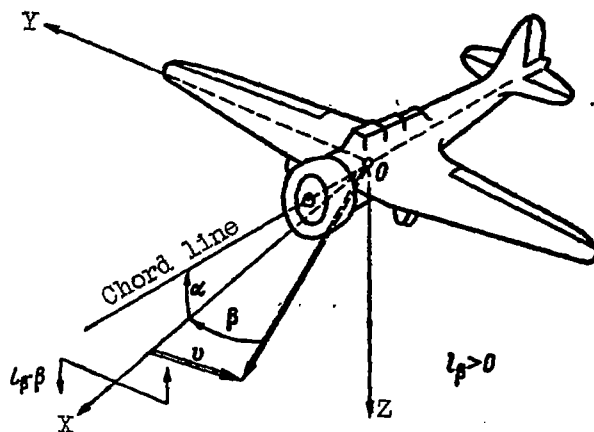
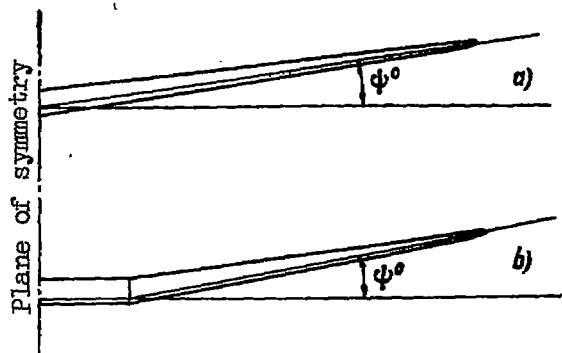
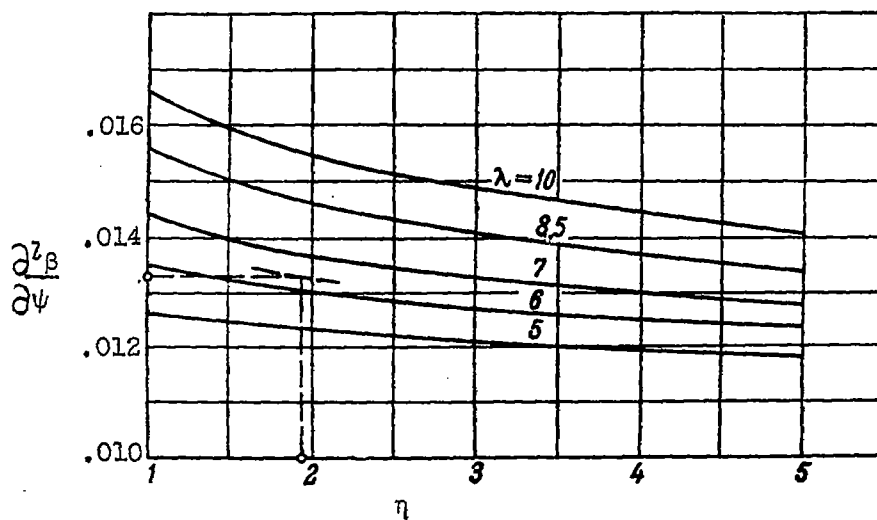
Figure 16. - Derivative  $l_{\beta}$ .

Figure 17. - Measurement of dihedral angle of wing (deg).

Figure 18. - Curves for determining derivative  $l_{\beta}$  of wing with dihedral.

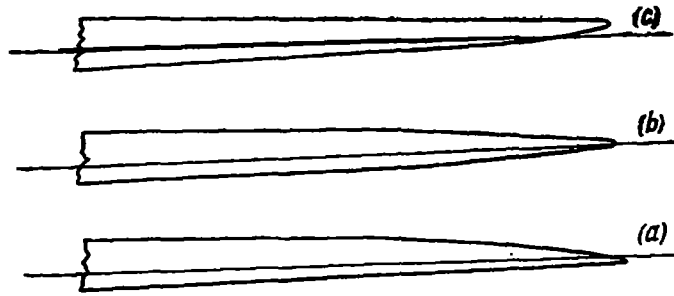


Figure 19. - Front view of wing tip.

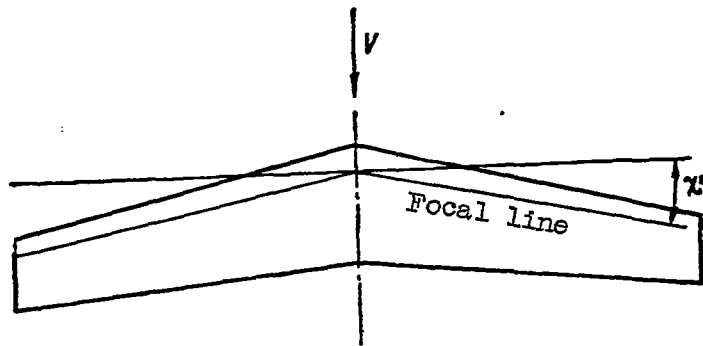


Figure 20. - Sweepback of wing.

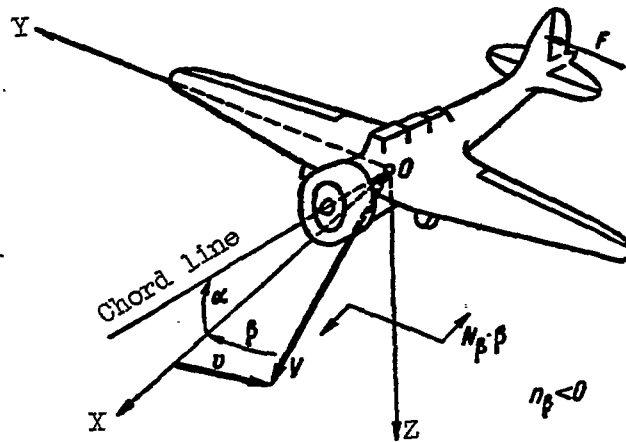


Figure 21. - Derivative  $n_\beta$ .

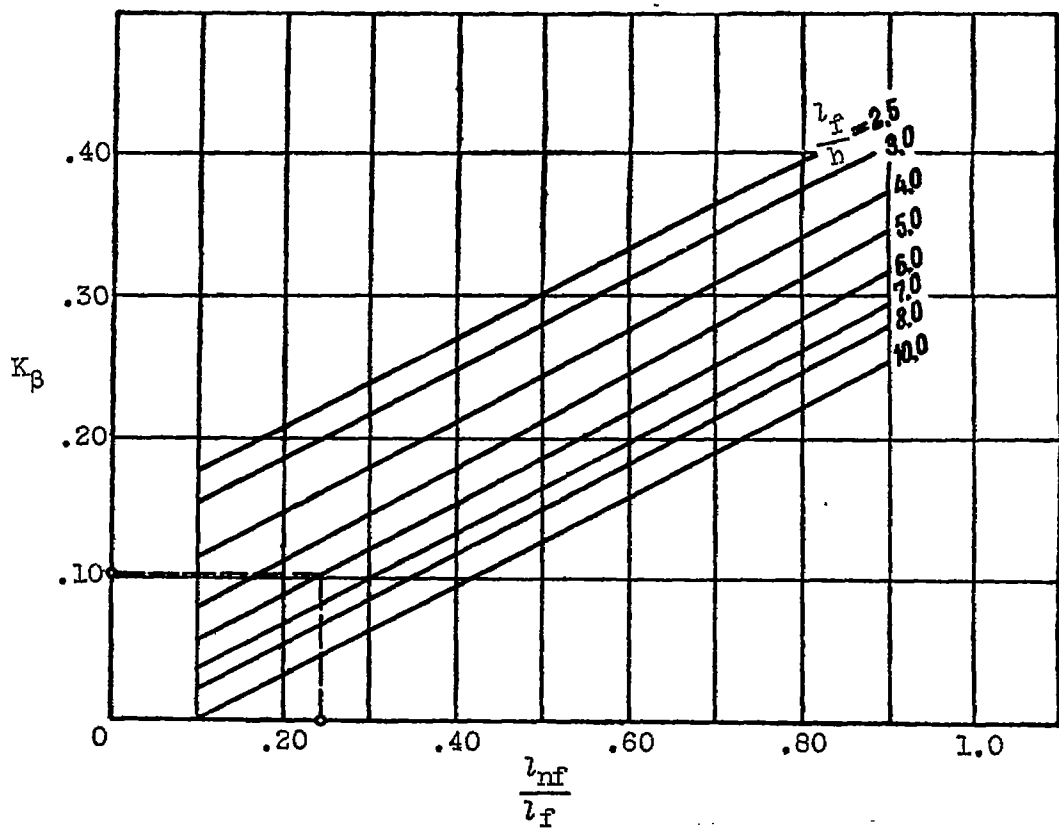


Figure 22. - Curves for determining effect of fuselage on derivative  $n_\beta$ .

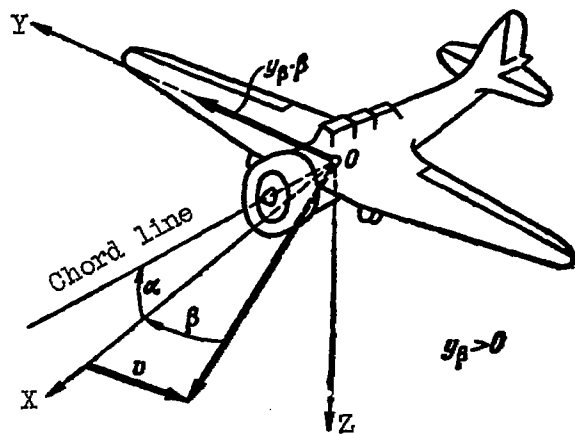


Figure 23. - Derivative  $y_\beta$ .

2014

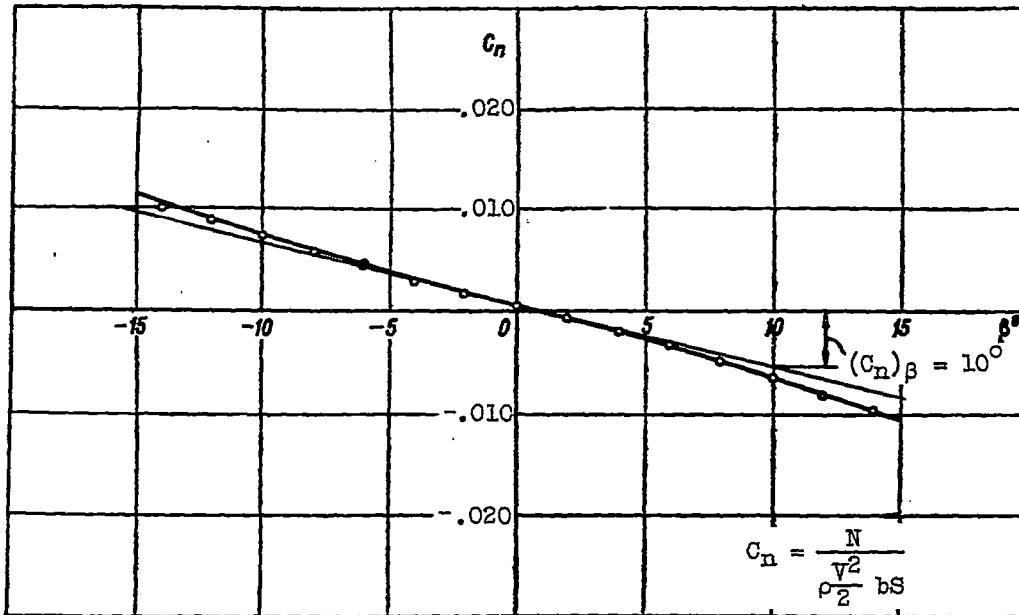


Figure 24. - Variation of yawing moment coefficient  $C_n$  with sideslip angle  $\beta$ .

$$n_\beta = \frac{\partial C_n}{\partial \beta} = \frac{(C_n)_{\beta=10^\circ} 57.3}{10} = \frac{-0.005 \cdot 57.3}{10} = -0.0286$$

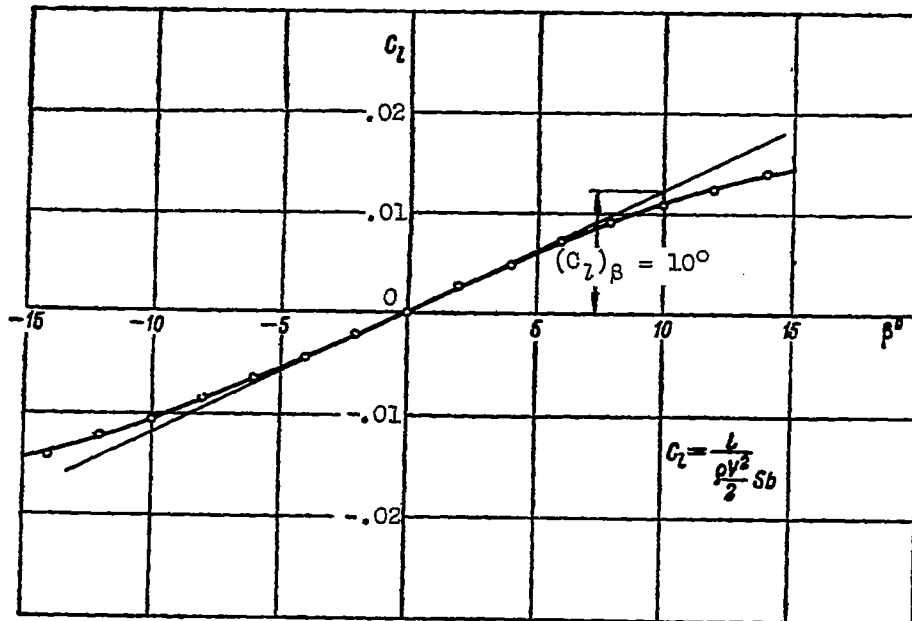


Figure 25. - Variation of rolling moment coefficient  $C_l$  with sideslip angle  $\beta$ .

$$l_\beta = \frac{\partial C_l}{\partial \beta} = \frac{(C_l)_{\beta=10^\circ} 57.3}{10} = \frac{0.0125 \cdot 57.3}{10} = 0.071$$

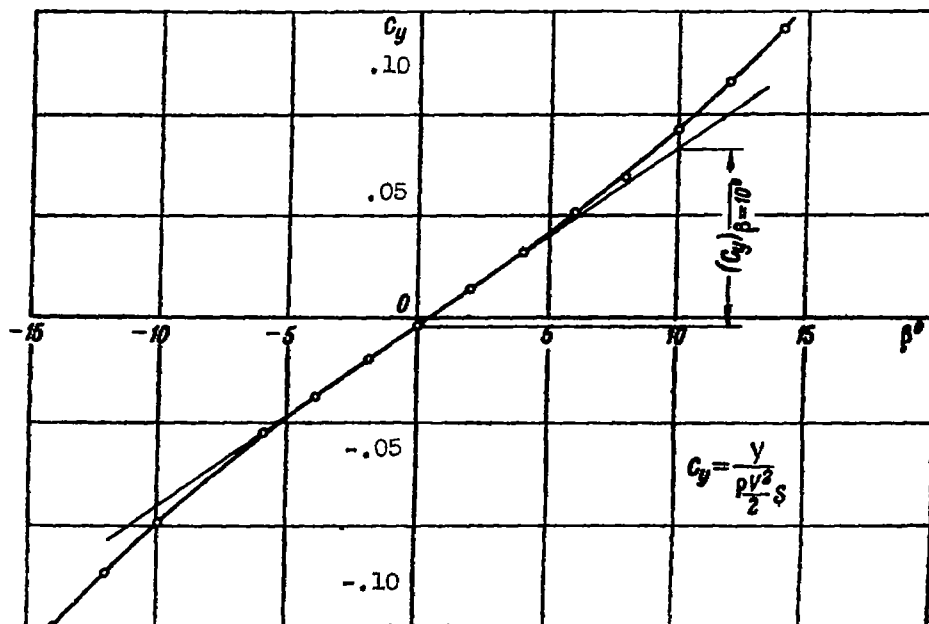


Figure 26. - Variation of lateral force coefficient  $C_y$  with sideslip angle  $\beta$ .

$$y_{\beta} = \frac{\partial c_y}{\partial \beta} = \frac{0.0825 \cdot 57.3}{10} = 0.5$$

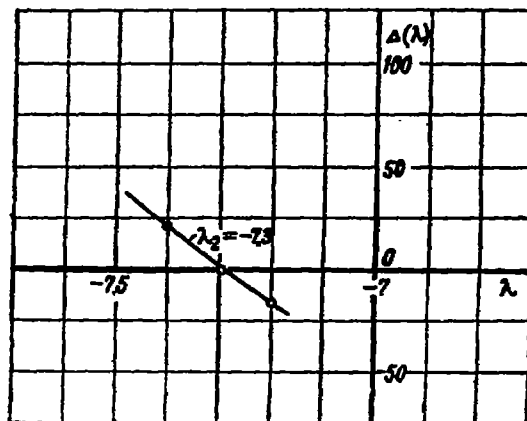


Figure 27. - Determination of root  $\lambda_2$  of characteristic equation.

2074

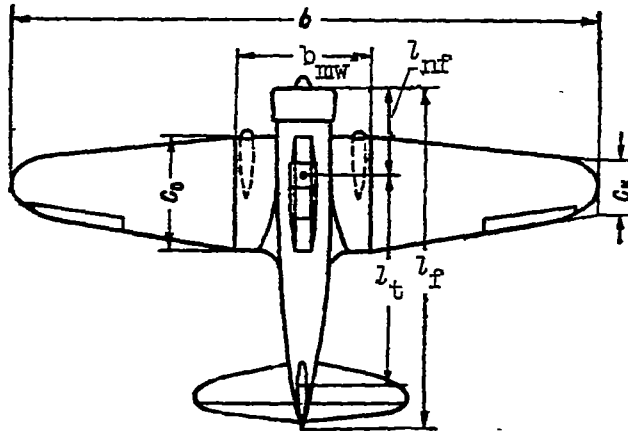


Figure 28. - Measurement of structural parameters of airplane.

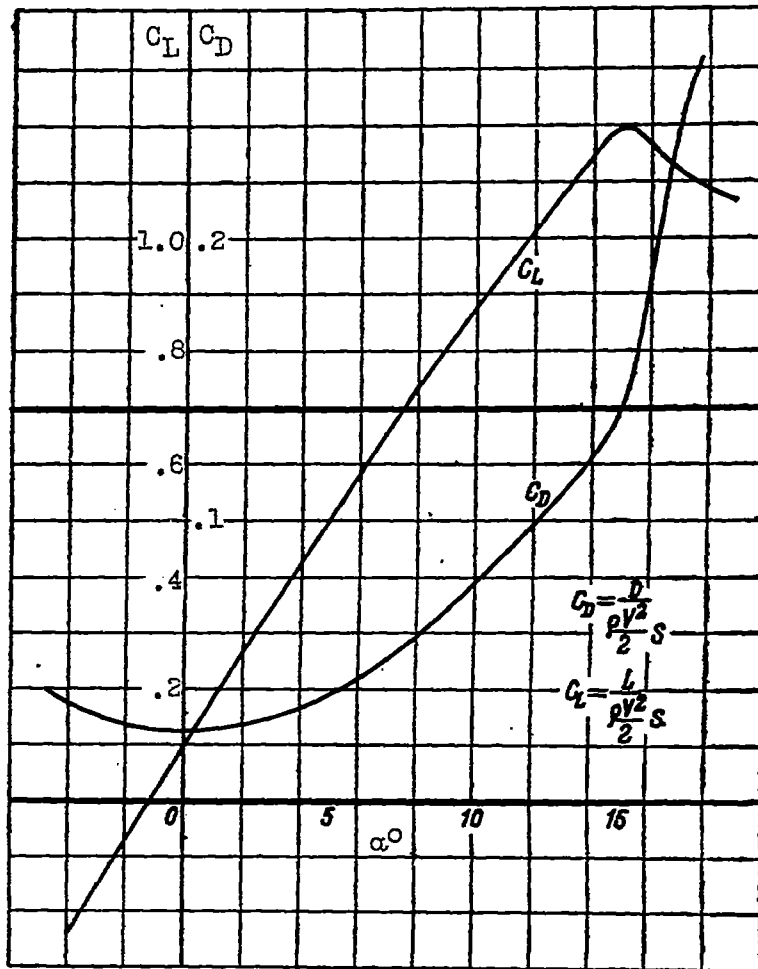


Figure 29. - Curves of lift force and drag against angle of attack.

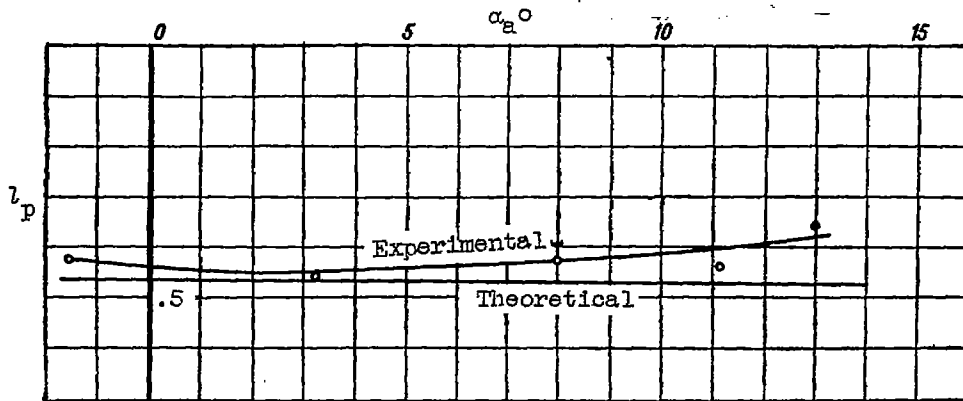


Figure 30. - Derivative  $l_p$  of Northrop airplane.

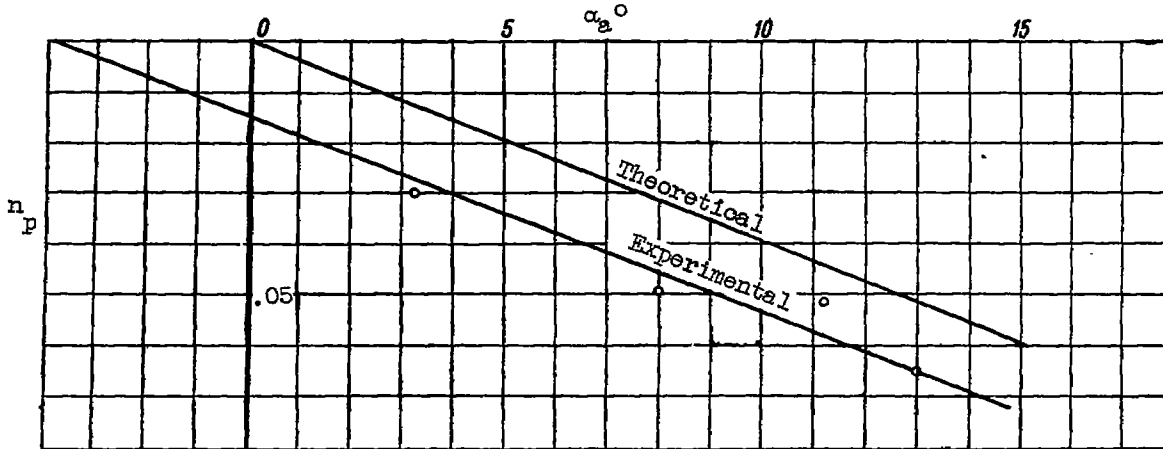


Figure 31. - Derivative  $n_p$  of Northrop airplane.

2074

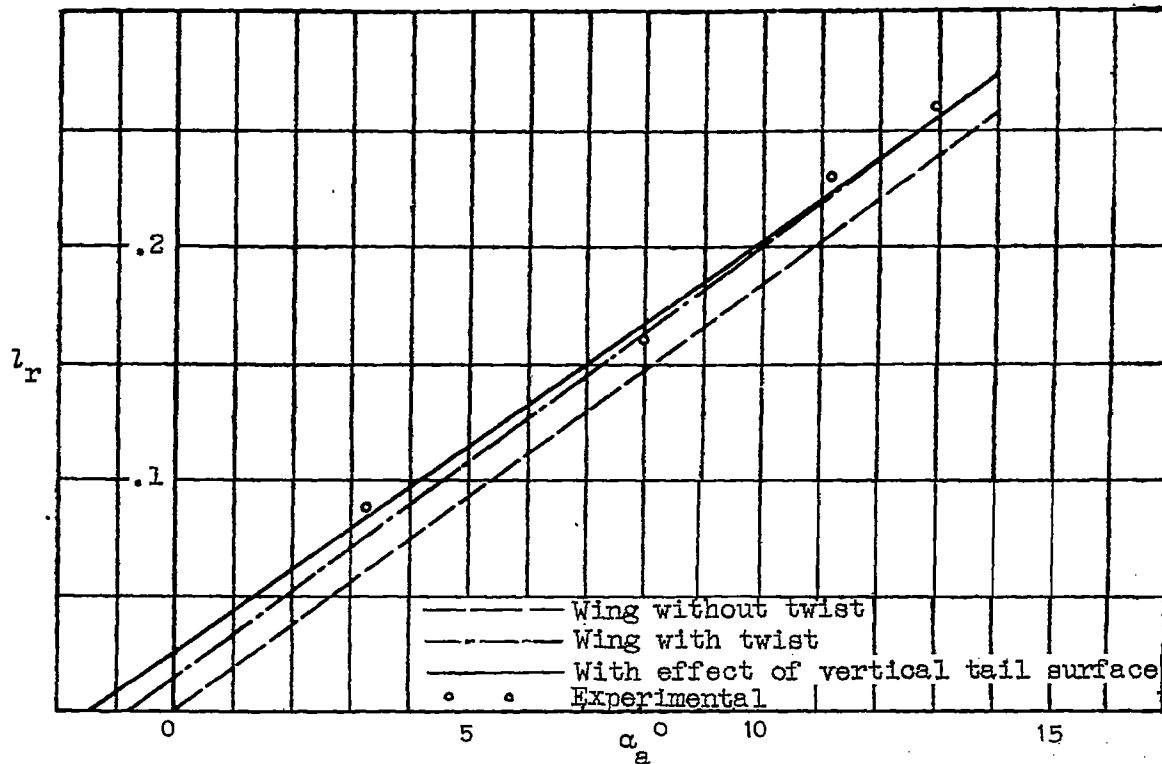


Figure 32. - Derivative  $l_r$  of Northrop airplane.

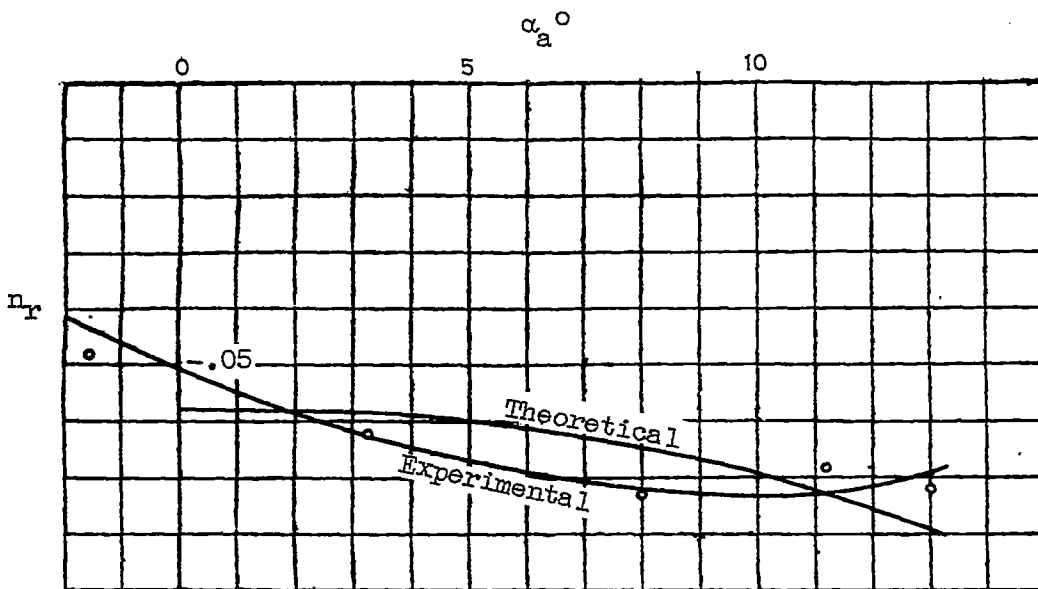


Figure 33. - Derivative  $n_r$  of Northrop airplane.

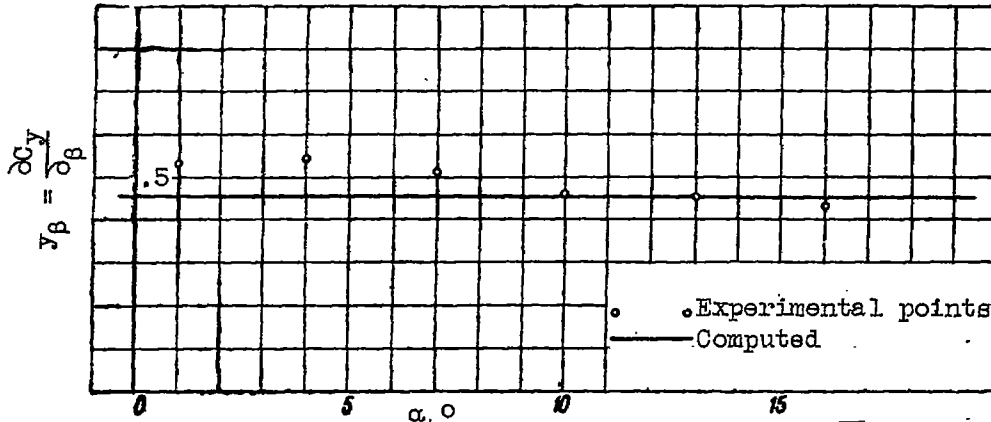


Figure 34. - Derivative  $y_\beta = \partial C_y / \partial \beta$ .

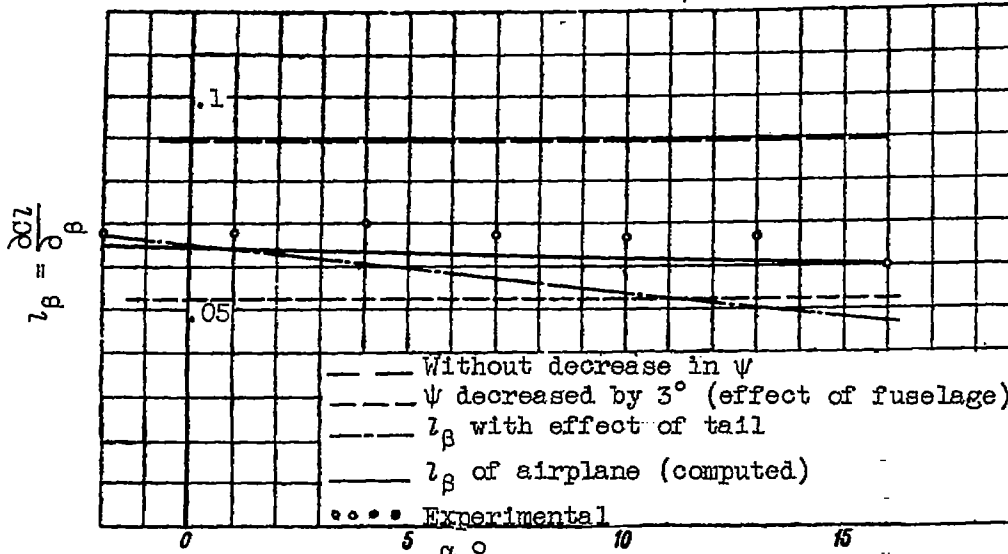


Figure 35. - Derivative  $z_\beta = \partial C_z / \partial \beta$ .

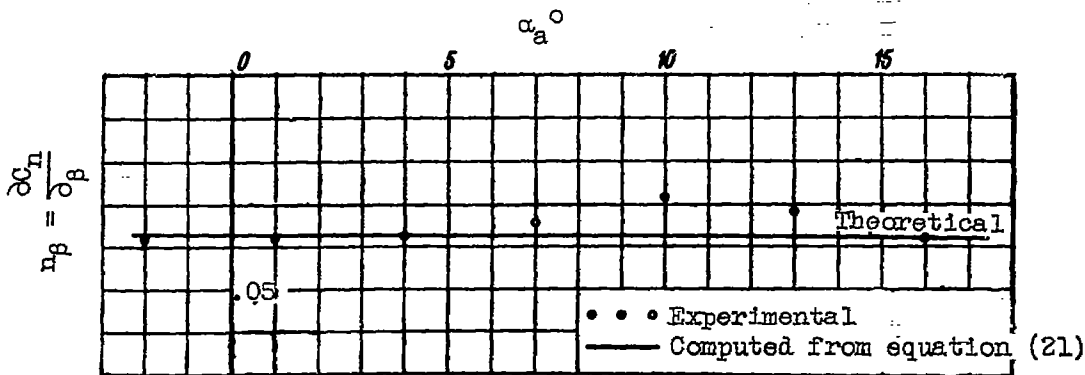


Figure 36. - Derivative  $n_\beta = \partial C_n / \partial \beta$ .

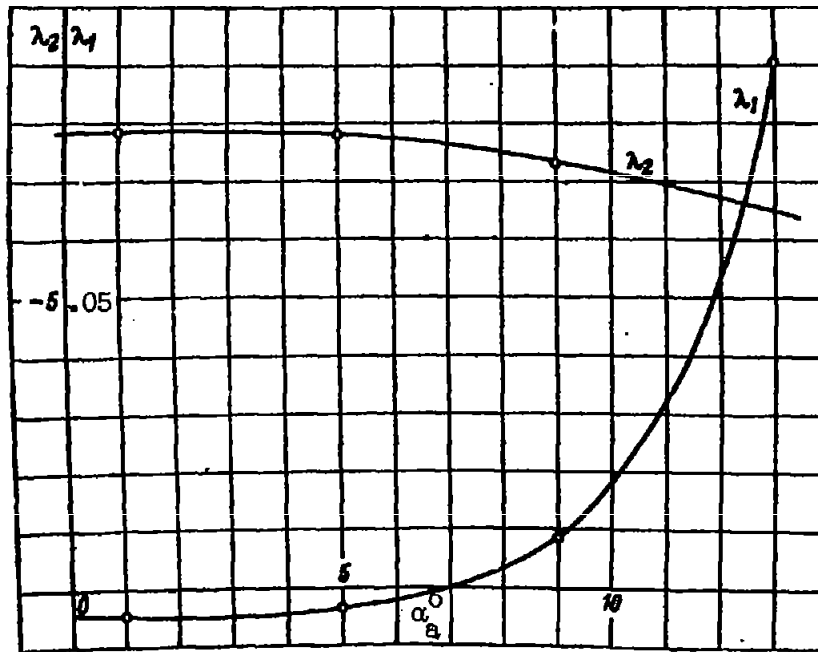


Figure 37. - Values of roots of characteristic equation  $\lambda_1$  and  $\lambda_2$  (Northrop airplane).

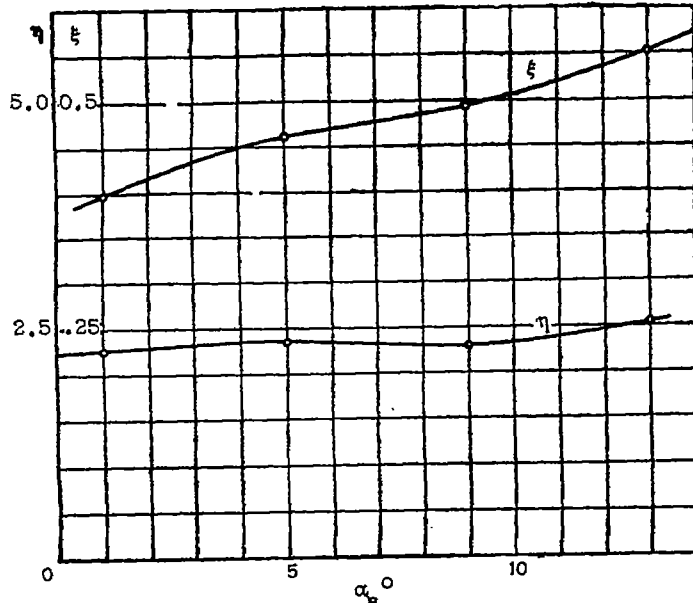


Figure 38. - Values of  $\xi$  and  $\eta$  (Northrop airplane).

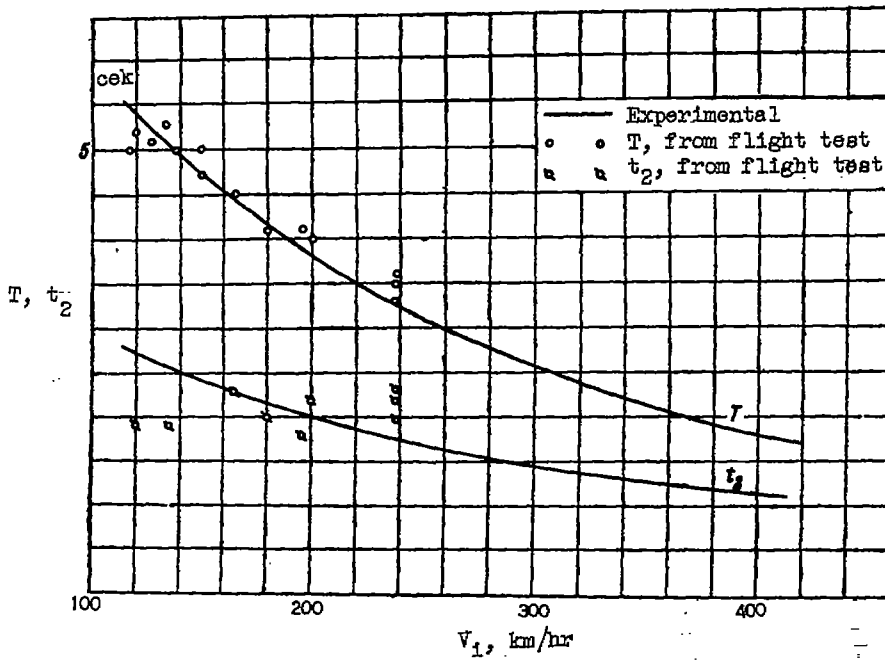


Figure 39. - Comparison of values  $T$  and  $t_2$  obtained by computation and from flight test (Northrop airplanes).